PEOPLE'S DEMOCRATIC REPUBLIC OF ALGERIA
MINISTRY OF HIGHER EDUCATION AND SCIENTIFIC RESEARCH
UNIVERSITY OF ECHAHID HAMMA LAKHDAR - EL-OUED
FACULTY OF TECHNOLOGY

Master's Thesis

In order to obtain a diploma of Master degree

Department: Mechanical Engineering

Specialty: Renewable energies in Mechanics

Theme

Zn-doped NiO Thin Films Deposited by Spray Pyrolysis Technique Using Solar Dish

Submitted by:

DJEGHBALA Okil

SAKER Baderddine

BERRETIMA Abdessettar

GHRISSI ALOUI Mohammed Salim

President	Mr. ZINE Ali	M.A.A	El-Oued University
Examiner	Mr. ATIA Abdelmalek	M.C.A	El-Oued University
Examiner	Ms. MEZIANE Assia	M.A.A	El-Oued University
Supervisor	Mr. MAAOUI Bedreddine	M.A.B	El-Oued University
Co-Supervisor	Mr. AOUN Yacine	M.C.A	El-Oued University

University Year : 2021/ 2022

Thanks

We thank, first, Allah the Almighty for having given us the will and the patience to carry out this modest work. We would like to express our sincere thanks to our supervisor Dr. MAAOUI BEDREDDINE

For his support, his orientation and his advice. Who have been very valuable to us.

We extend our heartfelt thanks to all Mechanical Engineering department teachers who have contributed to our training, particularly,

Dr. Khaled Mansouri, Mr. Abdeldjalil Laouini, Dr. Zine Ali, Mr.NID Abdelbaki

Finally, our thanks go to our families and friends from the University who have been many to help and encourage us.

DEDICATION

First, All thanks to God whose guidance and help allowed me accomplishing this humble work.

Secondly, I would like to express my gratitude to Mr. Abdelbaki NID for his patience, and assistance during writing this dissertation. Many thanks to my parents, siblings and mates who in a way or another helped me reach where I am now. And a special thanks to Dr. Housseyn Karoua for his help in my internship in CDER [Centre de Développement Énergie Renouvelable] I would also like to extend my thanks to the jury members for welcoming the review of this study , for providing scientific insights, and for evaluating this research study . A final thanks to our teachers throughout the five years of university for their academic guidance and help and a dedication to the memory and of my sister Ms. Fatma Saker May Allah bless her.

Table of Content

Liste of abréviations

***PVD** : Physical Vapor Déposition*
***CVD** : Chemical Vapor Déposition*
***APCVD** : Atmospheric Pressure Chemical Vapor Deposition*
***MOCVD** : Metal-Organic Chemical Vapor Deposition*
***PECVD** : Plasma Enhanced Chemical Vapor Deposition*
***MBE** : Moléculaire Beam Epitaxy*
***LPCVD** : Low- Pressure Chemical Vapor Deposition*

e_{HP} *: Demi-hauteur de la plaque chauffante (fil chauffant placé au centre)*	*[m]*
T_{HP} *: Température du fil chauffant*	*[°c]*
$e_{substrat}$ *: Hauteur du substrat*	*[m]*
T_{12} *: Température à l'interface plaque /substrat*	*[°c]*
$T_{substrat}$ *: Température à la surface du substrat*	*[°c]*
T_0 *: Température du milieu ambiant*	*[°c]*

$\varphi_{cond\,1}$ *: Densité de flux de conduction dans la plaque chauffante*

$\varphi_{cond\,2}$ *: Densité de flux de conduction dans le substrat*

φ_{conv} *: Densité de flux de convection entre le milieu ambiant et la surface du substrat*

***TCO** : Transparent Conductives Oxides*
***CDO** : Conductive Cadmium Oxide*

σ *: Conductivité électrique*	*[$\Omega^{-1}cm^{-1}$]*
μ *: Mobilité*	*[$cm^2/V.s$]*
***N** : Densité électronique*	*[cm^3]*
E_g *: Energie de bande interdite (Gap optique)*	*[eV]*
ε *: Constante diélectrique*	*[F/m]*

***LCD** : Liquid Crystal Display*

***dhkl** : Distance inter-réticulaire*	*[Å]*
***a** : Paramètre de maille*	*[Å]*

θ *: Angle d'incidence (angle de réflexion)*	*[degré]*
λ *: Longueur d'onde des photons X incidents*	*[Å]*
n *: Ordre de diffraction (nombre entier)*	
D *: Taille des cristallites*	*[nm]*
β: *Largeur à mi-hauteur de la raie de diffraction (ou FWHM)*	*[degré]*
α *: Coefficient d'absorption*	*[m-1]*
h *: Constante de Planck soit 6,63.10-34*	*[J.s]*
v *: Fréquence d'onde*	*[Hz]*
λEg *: Longueur d'onde correspondant au gap optique (Eg)*	*[Å]*
Eu *: Energie d'Urbach*	*[J]*
Rs *: Résistance surfacique*	*[Ω]*
: Résistivité électrique	*[Ω.cm]*
I *: Intensité du courant*	*[A]*
U *: Tension du courant*	*[V]*
ε *: Contrainte moyenne*	*[%]*
δ *: Densité de dislocation*	*[lines/m2]*
T *: Transmittance*	*[%]*
t *: Epaisseur*	*[nm]*

List of tables

List of figures

General Introduction

General introduction

Solar energy is considered one of the most important branches of renewable energy due to the availability of its main source, the sun, all over the world, which has led to the spread of solar energy use in most countries.

Solar energy, which can be used directly by humans for lighting (windows, skylights), heating and cooking (solar water heater, solar oven), is recently used to produce nanostructured thin films serving as substrates heater**.** Transparent and conductive oxides (TCO) are amazing materials in many ways. Their dual properties of electrical conductivity and apparent transparency make them prime candidates for optoelectronics, photovoltaics and electrochromic windows .[01]

The use of thin films is particularly attractive in industries where size reduction and low device dimensionality are required, such as the microelectronics industry [02]. Among the nanostructures, two oxides are used in this work, firstly zinc oxide (ZnO) which is an inorganic compound used in a number of applications. It is found in plastic rubbers, ceramics, glass, cement, lubricants, paints, ointments, adhesives, sealants, pigments, foods and batteries [03]. This oxide, in the form of thin films, can be developed at a temperature above 300°C. The second oxide is nickel oxide (NiO) which is an important material for use as dye-sensitized photocathodes and electrodes in alkaline batteries [04]. Also, it can be deposited at a temperature above 300 C°.

The objective of this thesis is the use of solar energy as source of heat, and deposition of Zn doped NiO at defferent Zn content (0,1,5 and 10 at %),and achieve the main characteristic properties of prepared thin films, such as structural, optical and electrical.

The thesis is structured as follows:

The first chapter includes the definition of the sun and its energy as well as its different applications and uses.

The second chapter is devoted to thin films with crystallographic, optical and electrical properties, with some applications, as well as the production and heating method used.

In the third chapter we discussed the tools used in the experiment and how to prepare the samples in the laboratory.

In the fourth chapter we analyzed and discussed the results obtained from the experiment.

Chapter I: Solar Energy and its Applications

I.1. Introduction*:*

The other new resources of energy is the renewable ones, and especially solar energy. In this chapter, we will present some general information about the solar energy and its applicability, like in generating electricity through the optical cells, also in the heating systems that can be used in cooking and other house needs...

This energy can also be used to produce thin films using the solar dish systems. The latter has a large number of electronic components and ecosystems In addition to optical links

I.2. The sun

The Sun as we know it, belongs to the main sequence of stars. It is in a state of hydrostatic (gravitation/pressure) and thermal (nuclear energy production/radiation)

(Production of nuclear energy/radiation), undergoing neither continuous contraction, nor dilation. The functioning of a star consists in finding a balance between the gravity which tends to crush it, and the pressure developed by the internal nuclear reactions. This equilibrium can be stable over a very long period (about ten billion years). The Sun is mainly composed of light elements such as hydrogen (92.1% of volume) and helium (7.8% of volume). It also contains, in lesser proportions, many other elements (oxygen, carbon, nitrogen, neon, silicon, magnesium, sulfur, etc.)]. The Sun has an internal structure and an atmosphere a section of the structure of the Sun is represented on .

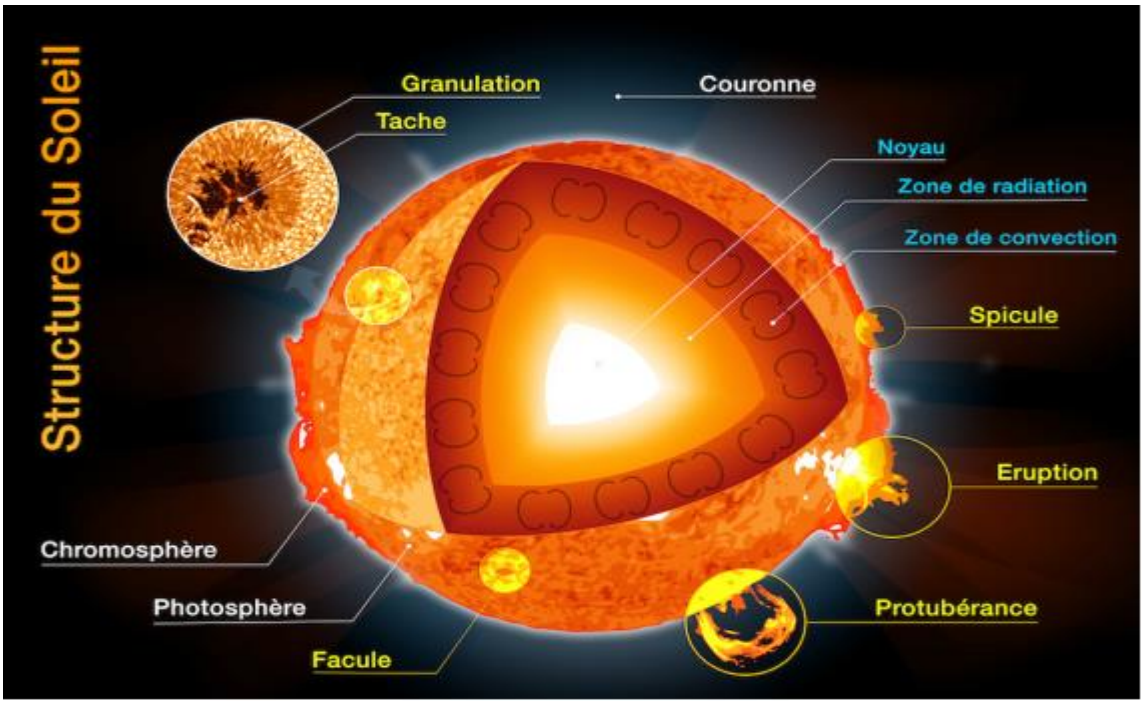

Figure 1 : *The internal structure of the sun*

The internal structure of the Sun is made up of several zones (the core, the zone of radiation and the zone of convection). At the heart of the Sun, is the core where the nuclear reactions take place. The radiation zone (or radiative zone) extends approximately tachocline is the zone of It is the separation zone between the radiation zone and the convection zone. It is located precisely at. Finally, the convection zone (or convective zone)

The atmosphere of the Sun is made up of several regions (the photosphere, the chromosphere, the corona and the heliosphere). The chromosphere is separated from the photosphere by the zone of minimum temperature and from the corona by a transition zone. The heliosphere extends to the limits of the solar system; it is a bubble-shaped zone elongated in space, generated by the solar winds.The Sun alone represents 99.86% of the mass of the solar system[05] .

I.3. Energy from the sun*:*

The Sun's energy is essential to life on the planet. Not only does it allow life to sustain itself, but it is also the origin of most of the energy used by humanity.also the origin of the majority

of the energy used by humanity. The Sun is the source of biomass, fossil fuels, and other renewable energies like wind and solar power. The solar energy is simply stored in a secondary form in fossil fuels. [06] Photosynthesis captures the sun's initial energy and preserves it in chemical bonds while the plants grow. After these plants have been transformed into fossil fuels, this energy is released millions of years later. All fossil fuels are basically composed of energy derived from energy derived from sunlight. Even after traveling hundreds of kilometers through the earth's atmosphere, solar radiation finally reaches the planet, carrying a considerable amount of energy. In general, the solar energy reaching the Earth at the surface of the upper atmosphere is about 1367 W/m2 at the present time.

The solar energy at the surface of the atmosphere is about 1367 W/m2 at full intensity [07]. [This power is about 340 W/m2, taking into account that only half of the Earth faces the Sun, as well as the varying amounts of sunlight that strike different latitudes and the volume of the atmosphere that the sun's rays must pass through.

The sun's energy not only produces electricity, but also heats the Earth to a habitable temperature (the structure of the atmosphere also contributes to the Earth's energy quota by maintaining a stable and by maintaining a stable and sustainable temperature). Weather patterns as well as ocean and air currents Ocean and air currents are all caused by the Sun . [06]

I.4. Some applications of Solar Energy*:*

There are two categories of technologies that harness solar energy, Solar Photovoltaics and Solar Thermal

I.4.1. Photovoltaic energy conversion :

Is a technology that converts sunlight (solar radiation) into direct current electricity by using semiconductors? When the sun hits the semiconductor within the PV cell, electrons are freed and form an electric current.

Solar PV technology is generally employed on a panel (hence solar panels). PV cells are typically found connected to each other and mounted on a frame called a module. Multiple modules can be wired together to form an array, which can be scaled up or down to produce the amount of power needed.

I.4.2. Solar water heating:

The solar water heating system (SWHS) is one of the most common application of solar energy utilization system. The usage of solar water heating system is not commonly employed throughout the globe, due to its high initial cost. The advancement in SWHS will lead to be beneficial over conventional system over the long span of time. The eco-friendly nature of such system promotes these systems to be used frequently in both domestic and industrial heating[08]

Figure 2 :*The solar water heating system*[09]

I.4.3. Solar- distillation :

Distillation is a process wherein a liquid or vapour mixture of two or more substances is separated into its component fractions of desired purity, by the application and removal of heat

The incident solar radiation is transmitted through the glass cover and is absorbed as heat by a black surface in contact with the water to be distilled. The water is thus heated and gives off water vapour The vapour condenses on the glass cover, which is at a lower temperature because it is in contact with the ambient air, and runs down into a gutter from where it is fed to a storage tank[10] .

Figure 3 : *Solar- distillation system*[11]

I.4.4. Solar pumping :

The solar photovoltaic based agricultural water pumping system is best suited technology for irrigation of farms. The generation of electrical power from Photovoltaic cell is mainly dependent on solar irradiations at respective times[12]

I.4.5. Solar furnaces:

A new high-flux solar furnace, capable of delivering up to 40 kW at peak concentration ratios exceeding 5000, is operational at PSI. Its optical design characteristics, main engineering features, and operating performance are described. This solar concentrating facility will be used principally for investigating the thermochemical processing of solar fuels at temperatures as high as 2500 K[13] .

I.4.6. Solar Thermal Power Production :

That utilize energy from the Sun to heat a fluid to a high temperature. This fluid then transfers its heat to water, which then becomes superheated steam. This steam is then used to turn turbines in a power plant, and this mechanical energy is converted into electricity by a generator. This type of generation is essentially the same as electricity generation that uses fossil fuels, but instead heats steam using sunlight instead of combustion of fossil fuels[14] .
These systems use solar collectors to concentrate the Sun's rays on one point to achieve appropriately high temperatures There types of systems to collect solar radiation:

I.4.7. Parabolic trough collectors (PTC):

Parabolic Trough Collectors (PTCs) are long parallel rows of curved glass mirrors concentrating beam radiation onto a receiver pipe located along its focal line.
The first practical experience with the parabolic trough concentrator dates back to 1870, when engineer John Ericsson designed and built a PTC collector with a surface area of 3.25 m^2 that was driving a small 373 W engine. From 1872 to 1875, John Ericsson built seven similar systems, but with air as working fluid. As shown in Figure 4, John Ericsson built a large solar engine in 1883 that was exhibited in New York. It consisted of a PTC with 3.35 m long and 4.88 m wide, focusing solar radiation on a boiler tube with 15.88 cm in diameter. The concentrator consisted of straight wooden moats, supported by curved parabolic iron ribs attached to the sides of the bowl. The reflective plates made of flat-silvered glass on the underside, were attached to these moats[15] .

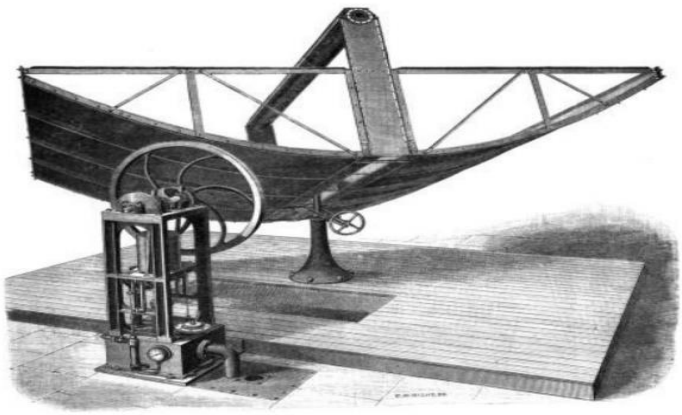

Figure 4 : *Parabolic trough collectors (PTC)*[15]

I.4.8. Heliostat field collector (HFC):

As shown in Figure 5, the heliostat field collectors (HFCs) consists of thousands of reflective mirrors equipped with a sun tracking system in two axes of rotation to focus the beam radiation on a central receiver placed at the top of the tower[15]

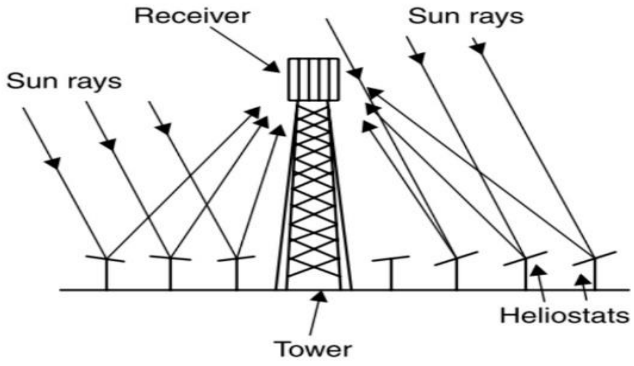

Figure 5 : *The heliostat field collectors*[15]

I.4.9. Concentrating linear Fresnel reflector (CLFR):

As shown in Figure 6, the CLFR operating principle lies in its flat mirrors, where each of these mirrors can be rotated following the sun path to constantly redirect and focus the beam radiation towards a receiver pipe, as the working fluid is heated while circulating in this horizontal tube.

This technology is named after the French scientist Augustin-Jean Fresnel, who invented Fresnel's objective in the eighteenth century for lighthouses. His idea was to grind a conventional convex lens on a multi-section lens to obtain a cheaper and lighter lens, which can send the light rays correctly in a given direction. The main idea of the LFR technology was inspired by the Fresnel lens to divide a parabolic mirror into a series of reflecting mirrors to focus the collimated rays on a focal point or line, depending on whether the reflectors are circular or linear[15]

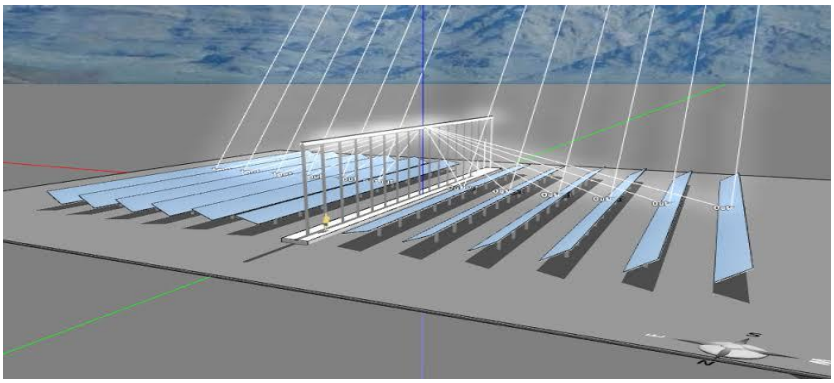

Figure 6 : *Concentrating linear Fresnel reflector* [16]

Figure 7 : *Parabolic dish concentrators* [17]

I.4.10. Parabolic dish concentrators (PDC):

The parabolic dish collectors (PDCs), they are small solar energy conversion units compared to other CSP systems (HFCs, PTCs and LFRs). The typical PDC system sizes are generally between 5 kW and 25 kWe. Figure 7 illustrates a PDC solar collector. For information, the largest parabolic dish collector has been designed and implemented in Australia with a reflective surface of 489 m^2 and a focal length of 13.4 meter. The major advantages of PDCs technology are :

- Possibility of installation on all types of ground without flatness constraint of the ground ؛
- Strong adaptation to stand-alone and isolated applications؛
- Modularity of the system and possibility of integrating thermal storage with high efficiency؛
- It has a high conversion efficiency compared to all types of concentrating solar systems (point and linear)[15] .

I.5. Solar dish systems*:*

The parabolic solar dish is one of the most important methods that use the sun heat as a source of generating electricity by concentrating the sun heat. Also in the current status, different thermal power technologies such as parabolic trough systems, solar tower systems, solar dish systems and linear Fresnel systems are used in solar power generation. The solar dishtracks the sun direction to focus the heat on the receiver, which drives a Stirling engine-generator unit. This technology has many applications in relatively small capacity applications (tens of kW) due to the size and the weight of available Stirling engines and wind loads effects on the dish reflector. The applications include generating electricity cooking, irrigation and water heating[18]

There are a lot of applications of solar dish system such as:

I.5.1. Electrical generation:

The main application of the solar dishes is to generate electrical power ranging from kW to MW. There are few researches dis-cussed some technologies to reach the optimal ranges for the solar dish systems as electrical generation. Wu et al[18] .

The solar-powered Stirling engine in Figure 7 coverts heat to mechanical energy by compressing working fluid when cold and allowing the heated fluid to expand outward in a piston or move through a turbine .

A generator then converts this mechanical energy to electricity.

I.5.2. Cooking:

Parabolic solar cookers use a parabolic-shaped reflector to direct sunlight to a small area in order to generate heat for cooking. They are able to reach high temperatures, 350 °C (662 °F) or higher, which allows them to be used for grilling and frying. These temperatures are significantly higher than what can be reached by a solar box cookers or solar panel cookers and allow the cooking times on a parabolic cooker to be comparable to a conventional stove, such as an electrical or gas burner[19] .

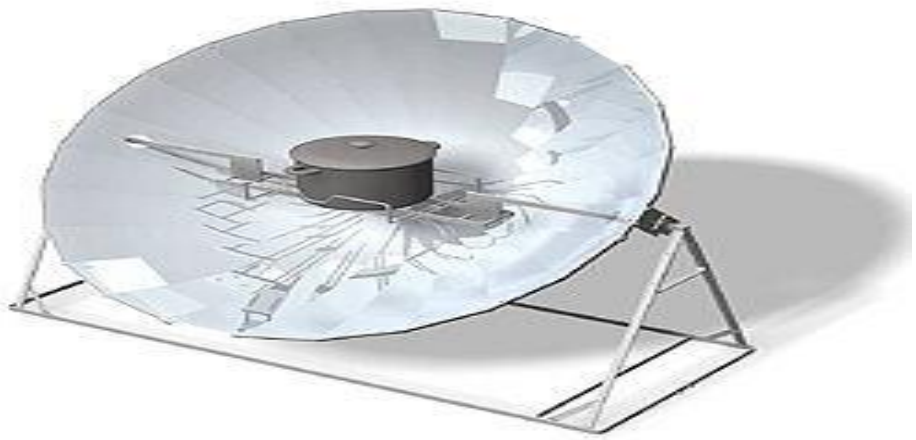

Figure 8 : *The parabolic solar cooker style* [19]

I.5.3. Water heating:

One of the most widely known solar thermal applications is the solar water heating system. Which uses natural solar thermal technology, where sunlight is converted into heat through collector, this heat transforms to water by using absorber tank[20] .

Figure 9 : *Solar water heater* [21]

I.5.4. Elaboration of thin films:

One of the most recent applications of solar energy is the production of thin films, in which the reflecting dish is used to produce heat by focusing sunlight on a glass plate and spraying the solution to be applied on the surface. In this case, the electric heater is replaced with a more ecologically friendly alternative[22]

I.6. Conclusion*:*

In this chapter, we started studying the structure, the characteristics and the the possible energy that we can get from the sun; through the dimensions, the effects and the different equipment required to provide a proper exploration of the solar energy, in addition to the possible way to produce the thin films.

In the second chapter, we are gonna take an exploratory study on the characteristics and effects of the thin films

Chapter II : Basics on Thin Films

I.7. Introduction:

This chapter offers a fresh perspective on thin films. It includes a description of thin films and an overview of their applications, as well as basic information on metal oxides and a brief discussion of methods for depositing these nanostructures. Finally, considers the spray pyrolysis process for thin film deposition that they would want to employ.

I.8. Thin film:

I.8.1. Definition of thin film:

A thin film is a material layer that ranges in thickness from fractions of a nanometer (monolayer) to several micrometers. The principal applications that benefit from thin film manufacturing are electronic semiconductor devices. The semiconducting material in thin film form is of particular interest since it has a wide range of uses.

Thin films play a significant part in the advancement of nanotechnology and nanoscience. Solar cells, which transform the energy of solar radiation into useful and constructive electrical energy, are an important application of thin film technology in light of the worldwide energy crisis. [20]

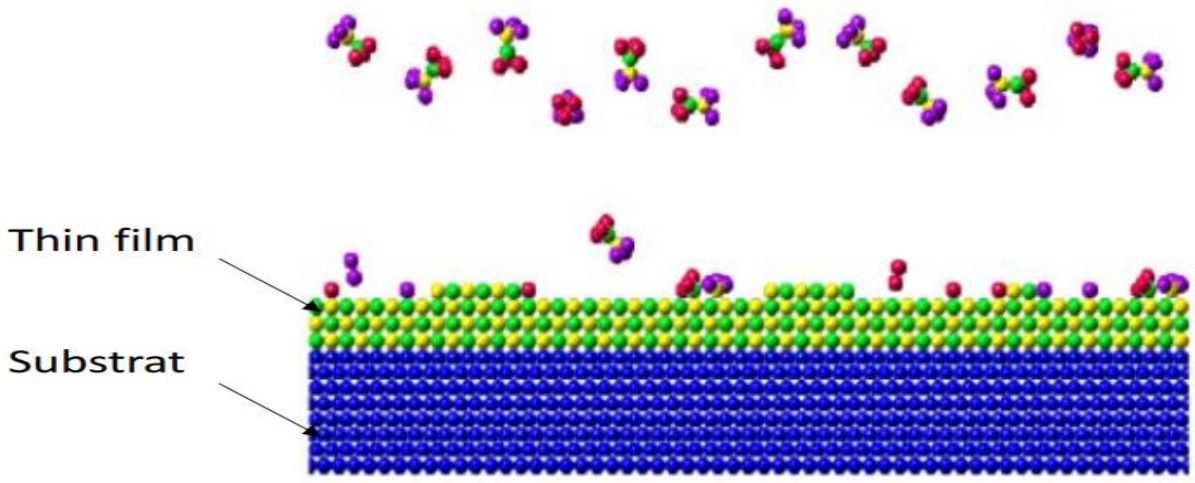

Figure **10 :** *Thin layer deposition on the substrate.* [23]

I.8.2. Applications of Thin Film:

The technology of thin film manufacturing has found applications in a large number of industrial sectors industry [figure 11], especially in the world of electronic components, sensors, optics or electronic components, sensors, optics or surface protection. [24]

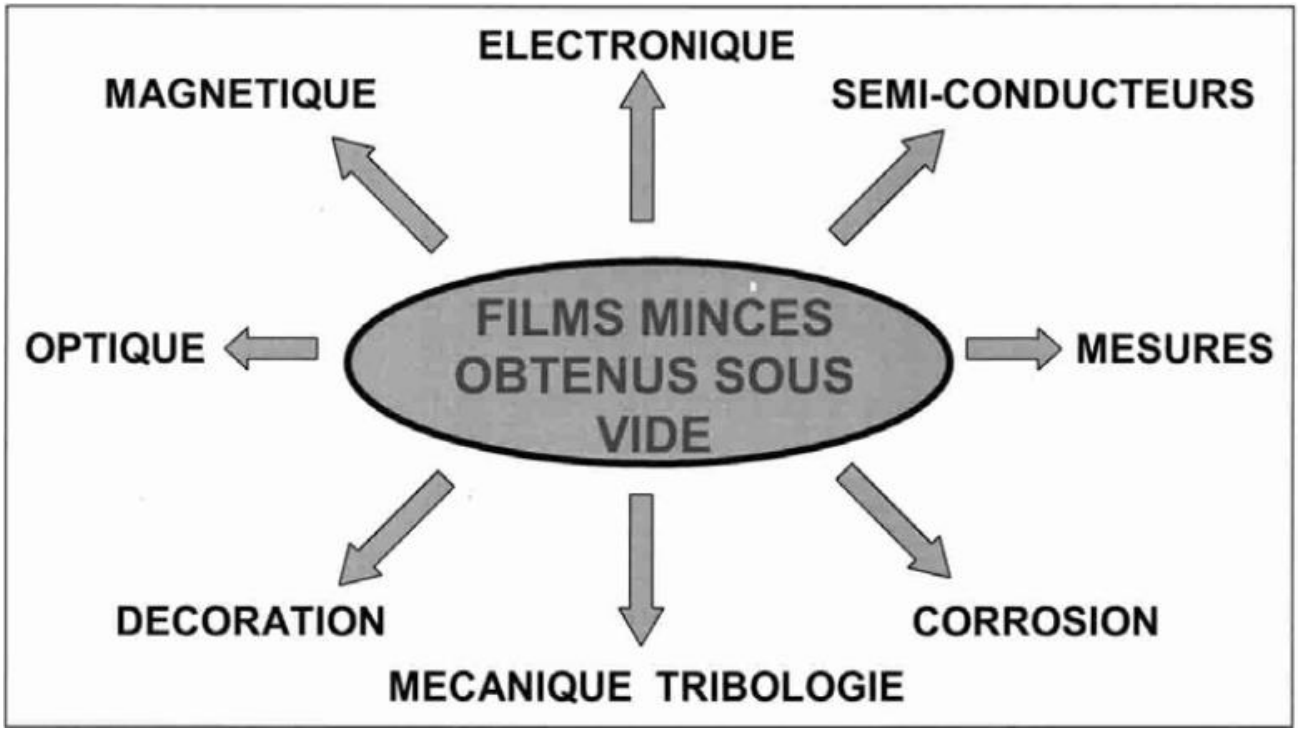

Figure **11 :** *Applications of thin films* [25]

In electronics, thin films are used for example for interconnections between various elements of a chip. For this purpose, thin layers of aluminum, gold or copper are used, which are good conductors and whose cost is relatively low. We can also use thin films in the heads of readings of hard disks. One uses then magnetic thin films. In optics, thin films are used to make anti-reflection films, for glasses or car windshields, or to make reflective films. In the same way, thin films can be used to create anti-corrosion surfaces that will harden the materials on which they are deposited, or even decorative surfaces. [24]

Presentation of materials:

I.8.3. Nickel (Ni):

Nickel is a transition element with atomic number 28 and symbol Ni.is a crystallized solid. Its molar mass is 58.69 g/mol, and its boiling point at normal pressure is 2730°C. The density is 8.9 g/cm^3, insoluble in water. [26]

I.8.4. Nickel oxide:

Nickel oxide is a transition material and antiferromagnetic. Their Neel temperature is 523K, a temperature that characterizes the Antiferromagnetic materials. Below this temperature the atoms of sub-networks spontaneously magnetize in the manner of a ferromagnetic network and its temperature of Curie temperature is about 2000K. [26]

Nickel oxide has an antiferromagnetic order which is related to the symmetry properties of the crystal symmetry (body-centered cubic structure, face-centered cubic,High chemical and thermodynamic stability, very resistant to oxidation).table shows some general properties of NiO. [26]

Table II.1 : *Some general properties of NiO. [27]*

Mean atomic number	**18**
Average atomic mass (g)	27.35
Molar mass (g/mol)	74.69
Boiling point (°C)	> 2000
Water solubility (mg/L)	1.1 At 20°C. insoluble
Melting point (°C)	1990 – 1960
Enthalpy of formation at 298k	-240 KJ/mole of atoms
Entropy S0 (JK-1.mol-1)	38.00

I.8.5. General properties of nickel oxide:

I.8.5.1. Structural properties:

Nickel oxide (NiO) crystallizes in a cubic structure of NaCl (rocksalt) type cubic structure shown in the figure 12. It has an elementary mesh with parameters
a = 4.117 Å, separated by an angle of 90°. It belongs to the space group Fm3m, in which the nickel atoms are in an octahedral coordination with six oxygen atoms, with a bulk density of 6.67g/cm3. [28]

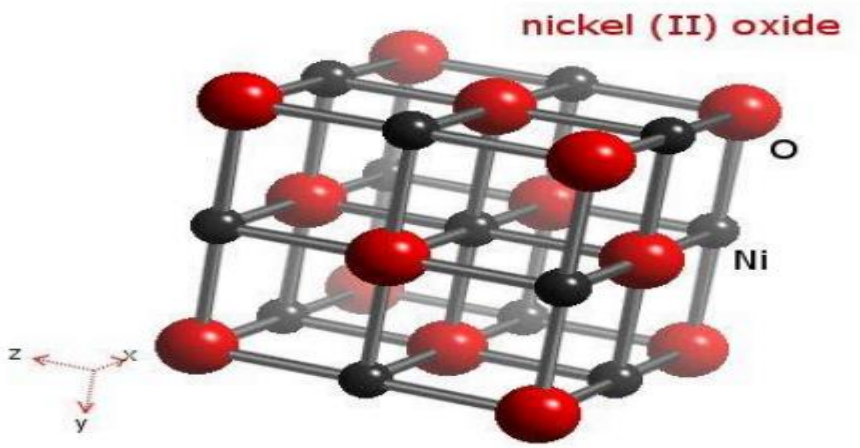

Figure **12 :** *Crystallographic structure of nickel oxide* [29]

I.8.5.2. Optical properties of Nickel Oxide:

Due to substantial absorption of violet (2.75 – 2.95 eV) and red 1.75 eV in transparent conductive oxides (TCO) with high conductivity and lighting gap energy directly, nickel oxide is green. The high absorption coefficient of the green spectrum (1.75 – 2.75 eV) grows in the presence of extra oxygen, especially when Ni is oxidized by straight oxygen or doping with Li+. Depending on the deposition process, the band gap of NiO thin films varies between 3.6 and 4 eV. To better understand the electrical composition of NiO, many optical tests such as photoemission or inverse photoemission trials have been carried out. Theoretical optical spectra computations have also been provided. [30]

I.8.5.3. Electrical Properties of Nickel Oxide:

Nickel oxide is a -P- type semiconductor with a wide energy gap of (3.6 - 4), and the charge carriers range from (10^18 - 10^19*cm*^-3) Therefore, it can be tailored to improve its electrical of the Therefore, it can be tailored to improve its electrical properties (improved electrical transport). [27]

Table II.2 : *Some electrical properties of NiO. [31]*

Conductivity σ (Ω. Cm)^-1	**≤ 0.1**
Mobility μ (cm2 / V. S)	0.1-1
Electron densities N (cm^3)	10^18 – 10^19
Band gap energy Eg (eV)	3.5 – 4ev
Dielectric constant	11.9

I.8.5.4. Applications of NiO:

Nickel compound has a variety of applications such as:

• In preparation of nickel cermet for the anode layer of solid compound fuel cells

• In metallic element nickel compound cathodes for metallic element particle microbatteries

• In electrochromic coatings, plastics and textiles

• In nanowires, nanofibers and specific alloy and catalyst applications

• As a catalyst and as anti-ferromagnetic layers

• In lightweight weight structural parts in part

• Adhesive and coloring agents for enamels

• In active optical filters

• In ceramic structures
• In automotive rear-view mirrors with adjustable coefficient of reflection
• In cathode materials for alkalic batteries
• Electro chromic materials
• Energy economical sensible windows
• P-type clear conductive films
• Materials for gas or temperature sensors, like CO device, H2 sensor, and aldehyde sensors
• As a counter electrodes. [20]

I.8.6. Zinc oxide (ZnO):

For many years, the main applications of zinc oxide have been in the chemical and pharmaceutical industries. Nowadays, new avenues of research in optoelectronics research are arousing great interest in this material because its properties are properties: high thermal conductivity, high heat capacity, medium dielectric constant high resistivity, low water absorption. It is important to note that in its pigmented form, it diffuses and absorbs strongly the ultraviolet radiations.

It is an attractive and promising material for many applications in surface acoustic wave devices (a VU), transparent electrode, blue and ultraviolet (UV) light emitters, solar cell windows, gas probes, photovoltaic device, chamber temperature ultraviolet lasers. [32]

I.8.7. General properties of Zinc oxide:

I.8.7.1. Structural properties:

Zinc oxide can crystallize in three forms: the hexagonal wurtzite structure, the zinc blende structure and the cubic rocksalt structure (NaCl),ZnO in the zinc-blende structure can only be stable if the film growth is on cubic substrates, the rocksalt structure can be synthesized at high pressure (above 10 Gpa at room temperature). Under ambient conditions Wurzite hexagonal is the most thermodynamically stable structure.

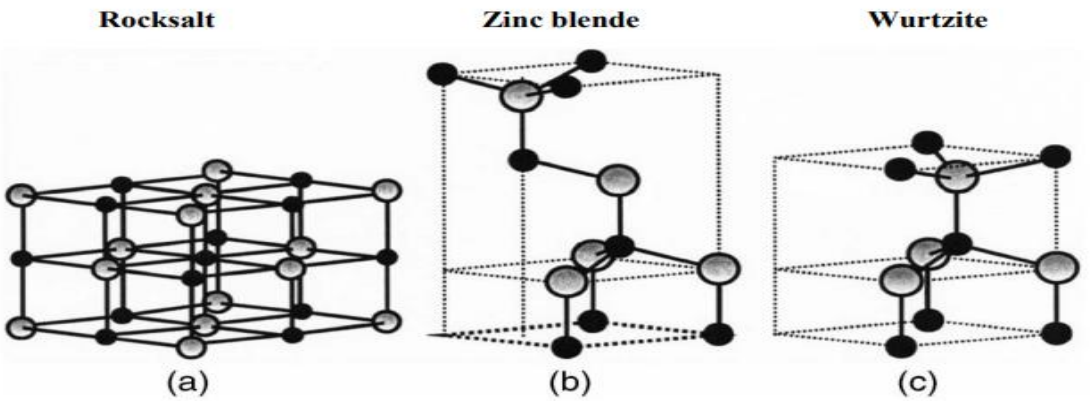

Figure **13 :** *Représentation des structures cristallines du ZnO : (a) rocksalt cubique, (b) zinc blende, (c) hexagonale wurtzite. Atomes de zinc en Gris ET oxygène en noir*

The ZnO crystal is characterized by the lattice parameters a = b = 3.24982Å and c = 5.20661Å in the Wurzite-type structure of space group P63mc, group number
186 in the Bravais classification, where the zinc and oxygen atoms are located in the positions:
Zn: 0, 0, 0; 1/3, 2/3, 1/2
O: 0, 0, μ; 1/3, 2/3, μ+1/2 with μ = 0,375

The simplest way to see the unit cell is to look at the tetrahedron represented on figure 14, whose base and vertices are constituted of four atoms oxygen. In fact, the zinc atom is not exactly in the center of the tetrahedron but displaced of 0.11 A° in a direction parallel to the c axis, to a certain extent, their individuality, contrary to what one would expect from a purely ionic purely ionic crystal. This phenomenon is due to the homopolarity of the Zn - O [33]

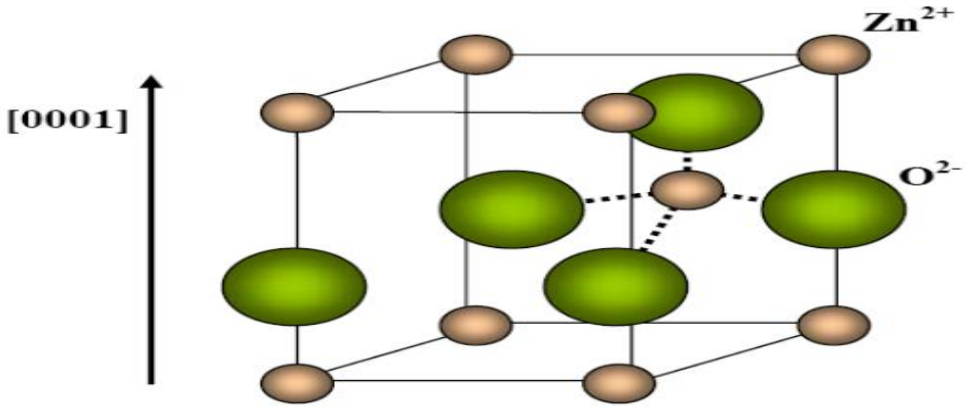

Figure **14 :** *Crystal structure of zinc oxide*. [28]

I.8.7.2. Optical properties and luminescence:

Zinc oxide is a transparent material with a refractive index in the solid form of 2. In thin film form, its refractive index and its absorption coefficient depending on the processing conditions the refractive index has a value which varies between 1.70 and 2.20 according to the authors. The improvement of the stoichiometry of ZnO leads to a decrease in the absorption coefficient and an increase in the energy of the band gap. Doped zinc oxide belongs to the class of transparent conductive oxides known as TCO (transparent conductive oxide). With very little doping, it can be used in luminescence.

Under the action of a high energy light beam (E > 3.4 eV) or electron bombardment, zinc oxide emits photons; this phenomenon corresponds to luminescence. Depending on the processing conditions and subsequent treatments, different photoluminescence bands have been observed:

They range from the near UV (350 nm), to the visible (green colored radiation with a wavelength near 550 nm). In stoichiometric thin films of ZnO, the visible luminescence is due to defects that are related to the emissions of deep levels, such as zinc interstitials and oxygen vacancies. Fons and al [33]. Reported that the study of the photoluminescence properties of layers in the visible region can provide information on the quality and purity of the material. [34]

Table II.3 : *Some optical properties of ZnO. [32]*

Dielectric constant	**ε // = 8.7** **ε ⊥ =7.8**
Absorption coefficient	10^4 cm^ -1
Refractive index at 560 nm	1.8-1.9
Refractive index at 590 nm	2.013-2.029
Exciton band width	60 meV
Transmittance	> 90%

As the luminescence depends on the doping of the material, this property is used in optoelectronic devices such as CRT displays, light emitting diodes for color display, signalling or lighting. Recently, the emission of ZnO layers has been intensively studied because of its high luminescent efficiency, its non-ohmic property and its high excitation binding energy (60 meV). This is higher than that of ZnS (20 meV) and GaN (21 meV) and moreover, ZnO can be prepared at a lower temperature than these two other materials.

I.8.7.3. Electrical properties:

A straight band gap exists in zinc oxide (E.g. 3.37 eV). is suitable for a wide range of optoelectronic applications. The valence band is made up of oxygen 2p levels, while the conduction band is made up of Zn 4s levels. Zinc oxide is usually n-type, and achieving p-type activity is extremely challenging. Any semiconductor will have defects and accidently added impurities, and zinc and oxygen vacancies (Vzn and VO, respectively) are the most common defects in ZnO, because the production energy for Vzn and VO is lowest for O-rich and Zn-rich circumstances, respectively. Zinc vacancies are a form of vacancy found in the zinc metal. [22]

I.8.7.4. Applications of ZnO:

Each attribute of ZnO has its own set of uses. ZnO is capable of generating clusters of ZnO nanocrystals and ZnO nanowires, starting with its band gap.

Due to its band gap, the synthesis of P–N homojunctions has also been recorded in several literatures. Many precise optical devices may be created reliant on the free-exciton binding energy of ZnO, which is 60 meV, since ZnO is stable at room temperature and above with a high exciton binding energy. Second- and third-order nonlinear optical behavior is seen in ZnO crystals and thin films, making them suitable for use in nonlinear optical applications. Generally speaking, tuning the physical characteristics of these oxides, such as zinc oxide, becomes the driving force behind the development of smart application devices. Cations with mixed valence states and anions with deficiencies can have their electrical, optical, magnetic, and chemical properties fine-tuned by permuting and combining their two basic structural traits (vacancies). The following diagram, Fig.15, summarizes the various ZnO implementations. [20]

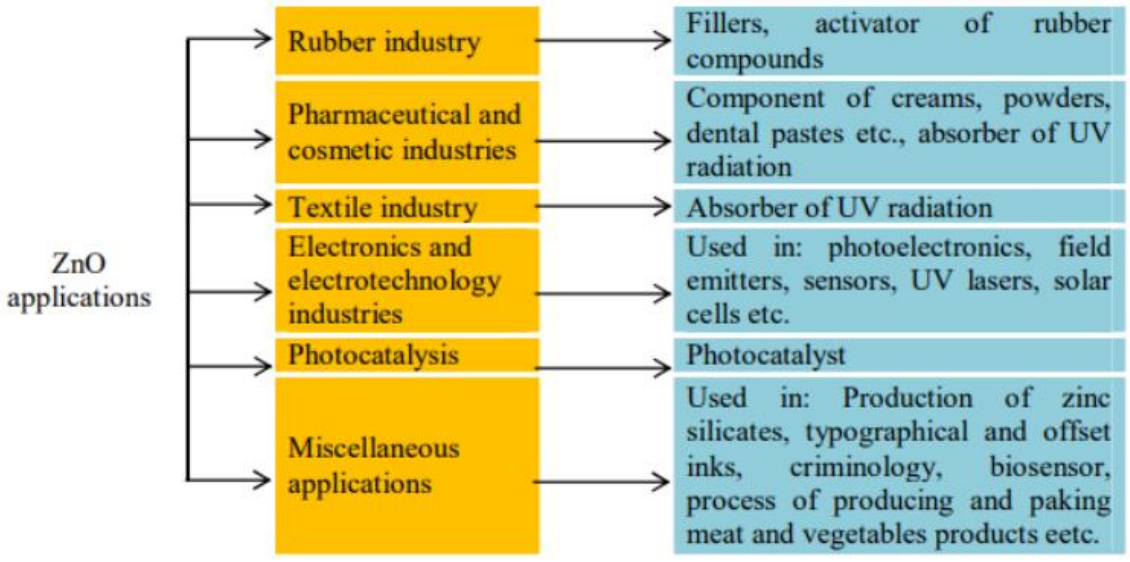

Figure **15 :** *Schematic representation the applications of ZnO.* [20]

I.9. Thin Film Deposition Techniques:

The main methods used to manufacture thin films in vacuum are chemical vapor deposition (CVD) and physical vapor deposition (PVD) [35, 36]. The classification of the methods is presented on the diagram of figure 16.

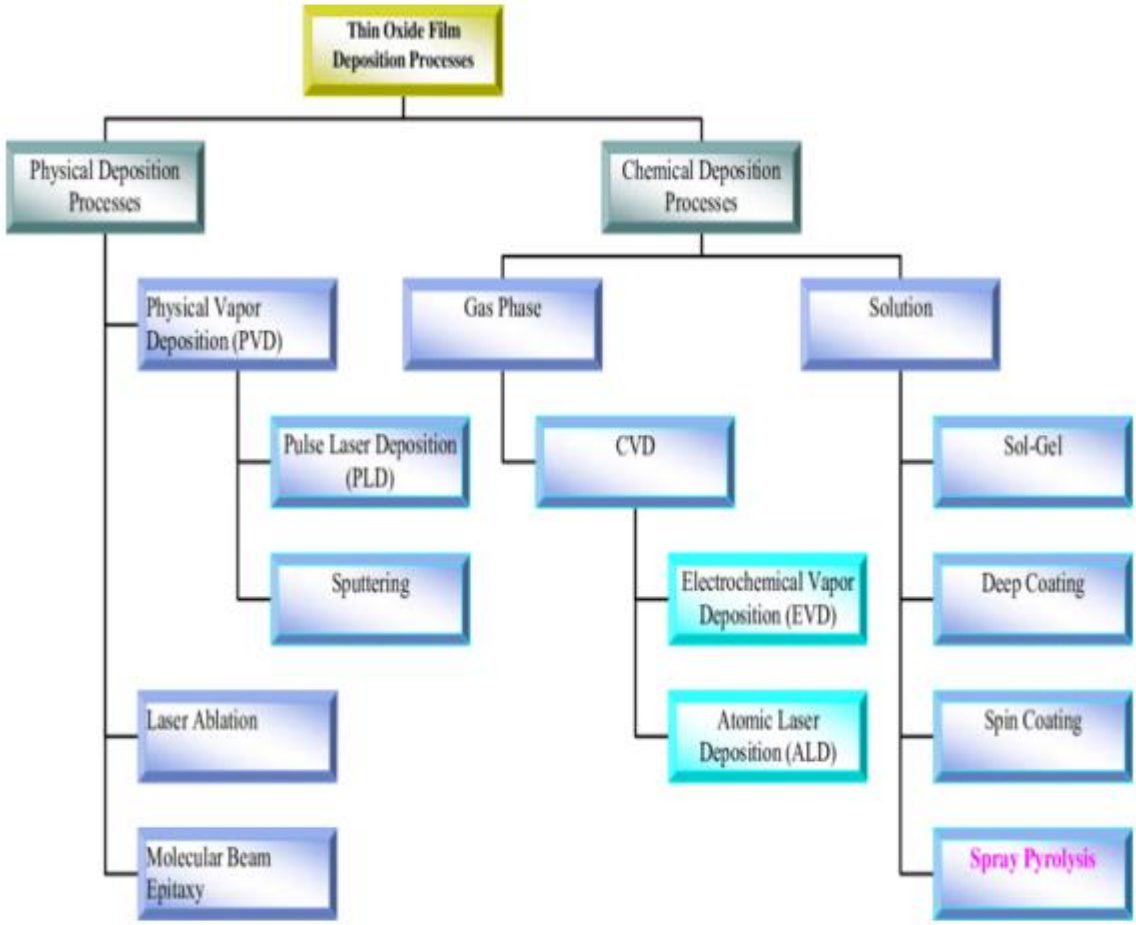

Figure **16 :** *The classification of deposition methods* [20]

I.9.1. Physical vapor deposition:

Generally, we can say that the deposits by physical vapor methods (P.V.D: Physical Vapor Deposition) are deposits elaborated generally by thermal evaporation, laser ablation and sputtering in all its forms.

We can summarize the main steps concerning these types of deposits as follows: the creation of the species (atoms, molecules...), then the step of transport of these species constituting the vapour phase towards the substrate and finally the condensation of the evaporated species on the substrate to form the deposit.

I.9.2. The different physical methods of elaboration of thin films:

The most known and usable methods are the following:

- Sputtering
- Vacuum evaporation
- Laser ablation
- Molecular beam epitaxy (MBE).

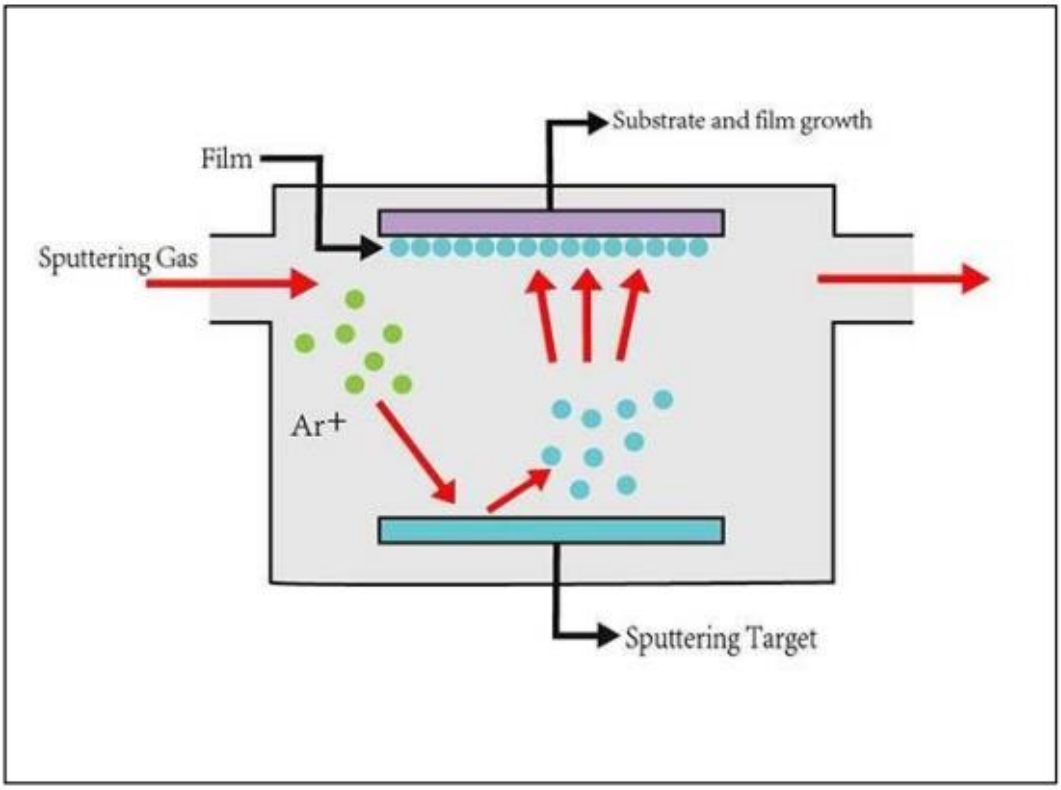

Figure 17 : *Physical vapour déposition méthode* [37].

I.9.3. Chemical vapor deposition (CVD):

Chemical Vapor Deposition (CVD) is a method in which the constituent(s) of a gas phase react to form a solid film deposited on a substrate.

The volatile compounds of the material to be deposited are eventually diluted in a carrier gas and introduced into a chamber where the substrates are placed [38].

The film is obtained by chemical reaction between the vapor phase and the heated substrate.

In some cases, an increase in temperature is required to maintain the chemical reaction. CVD is an interdisciplinary field, it includes a set of chemical reactions, a thermodynamic and kinetic process, a transport phenomenon. The chemical reaction is at the center of these disciplines: it determines the nature, type and species present. There are two types of reactors: the hot wall reactor and the cold wall reactor. In the case of the hot wall reactor, the latter is heated directly, which allows to operate at lower pressure: about 75 mtorr, for which deposits occur on the substrates, but also on the walls (LPCVD technique: Low- Pressure Chemical Vapor Deposition). In the case of the cold wall reactor, only the substrate is heated, so that the reaction is only effective at the of the heated substrate; it occurs at atmospheric pressure. The principle of this deposition method is presented in Figure 18, in the case of the hot wall [39].

As an example, the deposition of a highly refractory tungsten film can be done using a method described by the following equation:

$$WF_{gaz} + 3H_2\ gaz \xrightarrow{600°C} W_{solide} + 6HF_{gaz}$$

This formula implies that if two gases WF and H_2 are mixed, a tungsten layer can be obtained with the obtained with the CVD method.

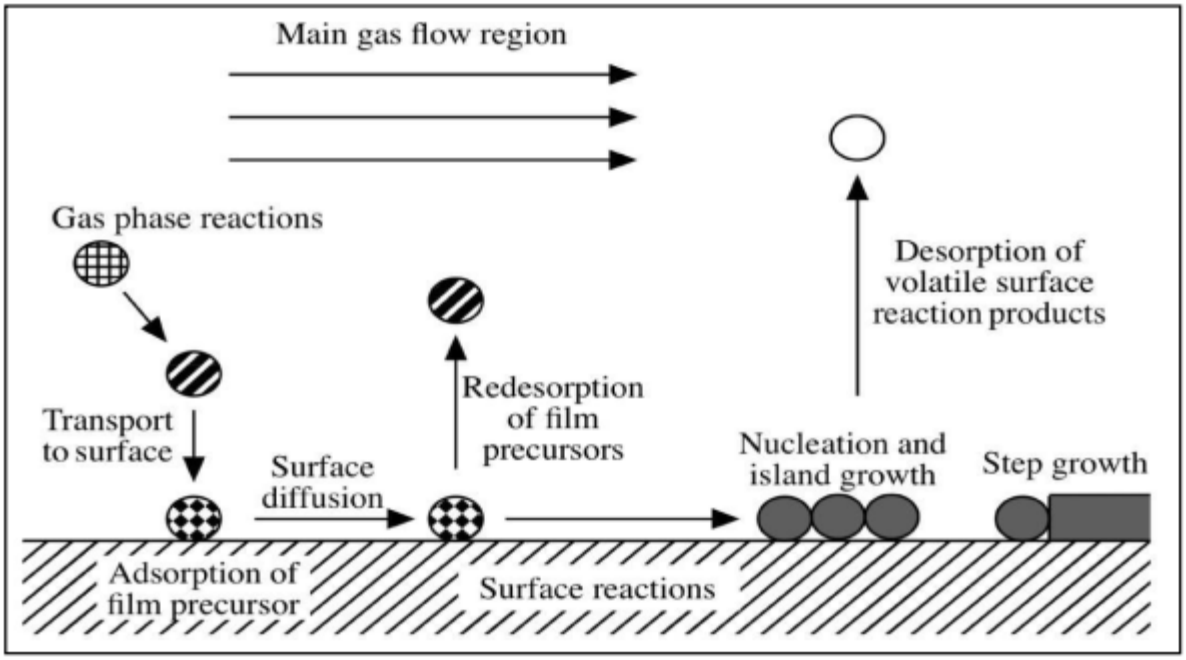

Figure **18 :** *Steps of chemical vapor deposition technique* [40]

I.9.4. The different chemical methods of elaboration of thin films:

The following deposition methods can be mentioned:

* Chemical Vapor Deposition (CVD):

There are several types of CVD techniques, we can mention: APCVD, MOCVD and PECVD.

* Solution Chemical Deposition:

- Electroplating (Electrodeposition)
- Sol-Gel process
- Spray pyrolysis method: this technique was used to prepare our thin films.

I.10. Spray Pyrolysis:

Spray pyrolysis is the most common name given to this technique. It is composed of:

Spray and pyrolysis.

Spray is an English word which indicates the jet of a liquid in fine droplets, launched by a sprayer.

For pyrolysis, we note that it has various definitions. The one that integrates the different descriptions is: "pyrolysis is a process by which a solid (or a liquid) undergoes, under the effect of heat and without interaction with oxygen or any other oxidants, a degradation of its chemical products to smaller volatile molecules".

This definition is identical to the thermal decomposition of a source to release a metal or a compound. [41]

I.10.1. General principle of the spray process:

A solution of different reactive compounds is vaporized and then sprayed, using an atomizer, onto a heated a sprayer, on a heated substrate. The temperature of the substrate allows the activation of the chemical reaction between the compounds. The experiment can be performed in air, and can be prepared in a chamber (or in a reaction chamber) under a vacuum of about 50 Torr.

This method based on the transfer of heat and mass, under unstable conditions, generates the displacement of droplets towards the substrate. These phenomena have, as consequences, changes in the size and composition of the droplet, which composes the reaction of the precursors.

The changes that the droplets undergo, after formation, can be summarized

as follows:

(a) Temperature changes, due to the temperature gradient between the nozzle (atomizer) and the surface of the substrate;

(b) Changes in velocity, due to the aerodynamic effect;

(c) Changes in size and composition caused by evaporation;

The point at which these transformations (changes) take place depends on the geometry of the equipment, the nature of the carrier gas and its flow, the solution and finally, the temperature profile between the nozzle and the substrate.

The description of the film formation by the Spray pyrolysis method can be summarized as follows:

(1) Formation of droplets at the nozzle outlet and evaluation of their average size.

(2) Decomposition of the precursor solution on the substrate surface.

Like any other thin film deposition process, the spray pyrolysis method also contains four (sometimes five) successive steps. Figure 19 illustrates, in a general way, the stages of the processes of elaboration of thin layers [42]:

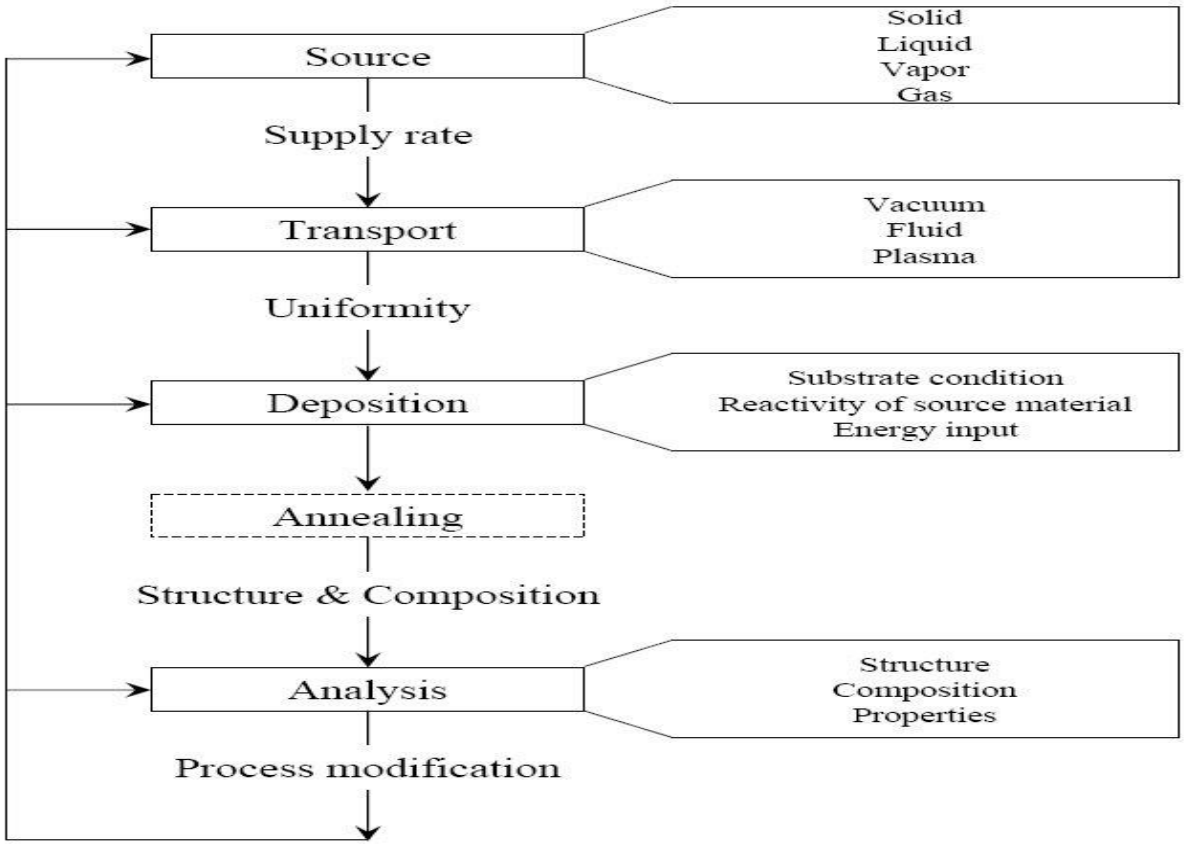

Figure **19 :** *Diagram of the steps of the thin film manufacturing process.*[43]

I.10.1.1. STARTING SOLUTIONS (SOURCE):

The composition of the final particle is determined by the dissolved bodies or reagents dissolved in the dissolver (starting solution) in a predetermined stoichiometric ratio. As precursors, usually inexpensive materials such as nitrates, chlorides and acetates are used, which are classified as reagents.

Distilled water or alcohol is often used as a solvent. In the basic solution it is necessary to eliminate the problems of solubility and phase segregation, where the different components precipitate at different times. To overcome this and to obtain homogeneous solutions, we recommend adding a small amount of acid (e.g. nitric acid) during the preparation. The overall concentration of the solution can be varied from 0.01 to some moles/liter. Note that this parameter has the effect of changing the average size of the fluid particles ejected.

According to the literature, some techniques include preheating of the solution. This preheating can, sometimes, be useful and promotes or accelerates the reaction on the substrate. This increases the deposition rate and improves the quality of the resulting films. [41]

I.10.1.2. DROPLET GENERATION (TRANSPORT):

The size and homogeneity of the deposited material can be roughly determined from the size of the sprayed droplets and the concentration of the solution while its morphology can also be determined by the concentration and velocity of the droplets produced by the atomizers.

Concerning the atomization or the identical way to the production of droplets and their dispersion in the air, several methods of atomization have been used in the studies spray pyrolysis, for example: pneumatic (air is the carrier gas), ultrasonic (pyro sol), gravitation, etc.

In the deposition device, the base solution can be transported to the substrate by the effect of a gas pressure. The gas pressure method has two advantages. Firstly, the flow can be controlled very sensitively and secondly, gases can also be used as secondly, gases can also be used as reactive elements in the composition of the material to be material to be deposited, in this case the semiconductor, such as O_2 for ZnO. However, for most compound

semiconductors, N_2 or an inert gas is used to avoid chemical reactions between the compound materials and/or the solvent, which would lead to the addition of addition of impurities. In some cases, in order to prevent the oxidation of the materials, a binary mixture of N_2 and H_2 is used as carrier gas. [42]

I.10.1.3. CHEMICAL REACTION ON THE SUBSTRATE (DEPOSIT):

When the aerosol droplets approach the surface of the heated substrate (200-600°C), under appropriate experimental conditions, the vapor formed around the droplet prevents direct contact between the liquid phase and the substrate surface.

This phenomenon occurs above a certain temperature, called the Leidenfrost temperature. This evaporation of the droplets allows a continuous renewal of the vapor, so the droplets undergo thermal decomposition and give the formation of strongly adherent film.

It is noted that the gas phase decomposition reaction of ZnCl2 occurring on the substrate surface is an endothermic reaction that requires relatively high temperatures for relatively high temperatures for the realization of the decomposition (pyrolysis) of the solutions used (droplets) arriving on heated substrates [41]:

$$ZnCl2 + H2O \rightarrow ZnO(s)\ depot + 2HCl\ (g)$$

I.11. Conclusion:

In this chapter, we discussed thin films. We also reviewed some of the uses of this layer, followed by a list analysis of zinc and nickel oxide, illustrating the structural, optical and electrical properties. We completed the chapter with a statement of the thin-film preparation procedures and a discussion of the spray change approach. In the next chapter, we'll look at our elaboration method, which uses solar energy as a heat source and allows us to avoid classification methods.

Chapter III : Growth Process and Characterization methods

I.12. Introduction

Spray pyrolysis involves atomizing a precursor solution to produce an aerosol, which is then sprayed onto a heated substrate to form a thin layer. This technology is used to make a thin layer with robust characteristics in a variety of surface applications. Spray pyrolysis offers a number of advantages, including its low cost, the fact that it just requires basic deposition tools, the capacity to fabricate large-area films quickly, and the ability to execute molecular doping. Are particularly well suited to the production of oxide thin films. This chapter begins with a description of the experimental settings and a quick review of the Experimental instruments of a handmade SPT system. The second section delves into the exact characterisation procedures needed to establish each layer's structural, optical, and electrical characteristics.

I.13. Elaboration technique

I.13.1. Experimental montage used

It is a frame realized in the technological Hall of the department of mechanical engineering of the University of ElOued. It is built from simple devices to which we made some modifications in order to realize homogeneous films of metal oxide. The diagram of the system of deposit conceived and carried out is shown on figure 20

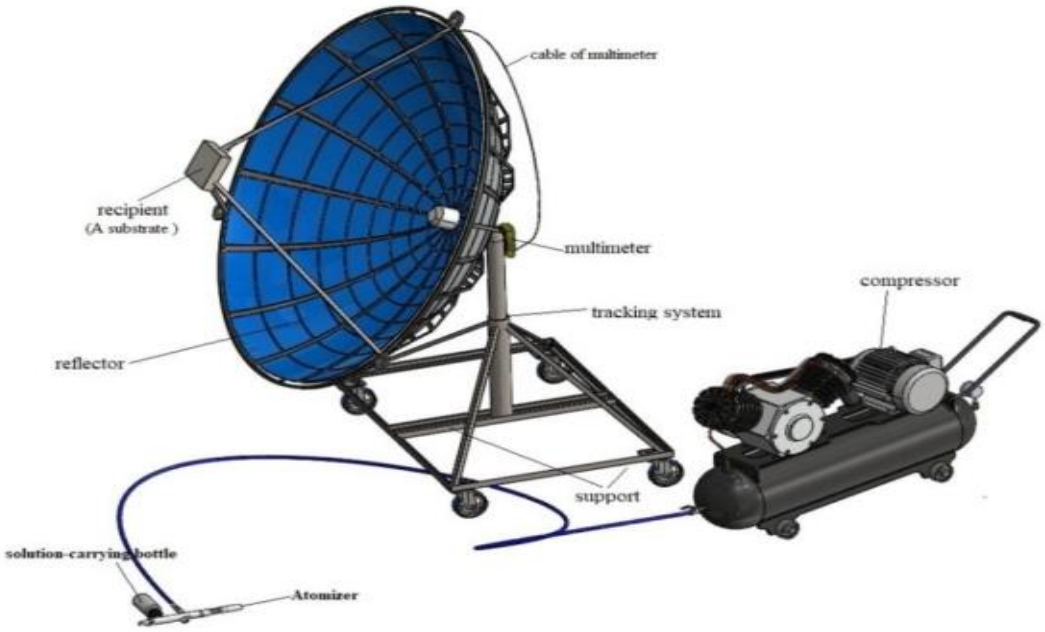

Figure **20 :** *Full experimental system assembly. .(Designed by Solidworks)* **.**

I.13.2. Description of the elements of the device

The objective of our work is first of all the realization of a system of deposition of thin layers by the technique of spray and its optimization by the study of the effects

by the spray technique and its optimization by the study of the effects of the deposition parameters on the quality of the films.

The main elements of the device are :

- **A reflector** ; It is a satellite receiver dish covered by a hundred small mirror surfaces that cover the inner surface of the reflector.surfaces of mirrors that cover the inner surface of the reflector. The mirrors should have their shiny side facing the sun.

- **A substrate holder** ; it is a 15cm long plate, heated by solar energy, whose temperature can be temperature can be regulated manually using a multimeter type (VCA61A - LCD).

This temperature can be varied and increases up to 500°C.

- **Atomizer (aerosol)** ; It is an element that transforms the solution into droplets. It is placed on It is placed on a support with adjustable height in order to control the distance between the nozzle and the substrate.

- **Air compressor** : It is a device that provides pressure to the atomizer in order to operate it.

I.13.3. Oven temperature measuring instruments :

We used a digital multimeter (VCA61A) whose characteristics are the following (figure. 21):

- Model VCA61A - LCD 10fct,

- Operating range K. 0 - 1300 °c,

- Power supply; a single battery (9 V).

Figure **21 :** *Photo of the digital multimeter used (VCA61A - LCD)*

I.13.4. Experimental conditions :

The ideal operation of the oven is when the solar radiation is parallel to the axis of the focus. We have period where our device is in a clear sky environment, in effect of shadows.

I.13.4.1. Setting the oven :

The oven is oriented towards the sun. With the help of a controlled tracking system. It is redirected to the position of the sun since its rise. The solar rays are reflected at the focus of the The sun rays are reflected at the focus of the paraboloid, forming the sun spot that should appear on the front of the plate to be heated.

I.13.4.2. Multimeter location :

To measure the temperature reached on the oven surfaces, the multimeter probe is placed on the receiver surface (Figure 22):

Figure **22 :** *Position of the multimeter probe.*

I.14. Experimentation :

I.14.1. Choice of the deposition substrate :

The substrates used are glass slides with a surface of (7.6 x 2.6) cm2 and a thickness equal to 1 mm, cut by a diamond-tipped pen. This choice of glass is due to two reasons:

It allows a good optical characterization of the films and is well adapted for its transparency and its important theoretical expansion coefficient giving a good adhesion of the deposited layers.

After deposition, the sample (substrate + layer) is cooled from the deposition temperature to room temperature (~20 °C) which causes a compressibility of the two materials constituting the sample. In this case, they have very close coefficients of expansion, hence a minimization of the stresses. It should be noted that the increase in temperature of the substrate leads in the increase of the stresses. This is related to the compressive stress caused by the difference between the expansion coefficients of the substrate and the deposited material (α glass = $8.5 \times 10^{-6} k^{-1}$, $\alpha\ NiO = 7.93 \times 10^{-6} k^{-1}$) [29] and also for economic reasons.

I.14.2. Preparation of the substrates :

The quality of the deposit and consequently that of the sample depends on the cleanliness and condition of the substrate. The cleaning of the substrate is therefore a very important step. and dust and check by eye that the surface of the substrate is free of scratches and defects in flatness. These conditions are essential for the good adhesion of the deposit on the substrate and for its uniformity (constant thickness).

To perform an optoelectrical study of NiO and Zno thin films, we used glass substrates in order to achieve a clean thin film deposition; it is To do this, it is essential to go through the cleaning process of the substrates because the electrical characteristics are very sensitive to the surface preparation techniques.

The process of cleaning the surface of the substrates is as follows:

- The substrates are cut with a diamond-tipped pen.
- Degreasing in a trichloroethylene bath for 5min.

- Rinsing with distilled water and then with acetone for 15 min.
- Rinsing with distilled water.
- Washing of the substrates in methanol at room temperature in an ultrasonic bath to remove traces of grease and impurities stuck to the surface of the substrate then they are cleaned in a distilled water ultrasonic bath.
- Drying with a dryer. Avoid touching the surface of the substrate, to avoid any contamination.

I.14.3. Preparation of the precursor solution and deposition condition :

Two oxides (ZnO and NiO) were deposited in this pilot work, and for ZnO, we will deposit three chains and choose the influence of different deposition coefficients existing in one or more states. We picked another modulus effect in NiO since it has comparable qualities to ZnO.

➢ **Zinc oxides**

In 100 mL of water, 0.1M Zinc acetate dihydrate (Zn(CH3COO)2,2H2O) was used to make the ZnO solution. Drops of HCl can be introduced to the solution as a stabiliser for heating when the solution is put on the heater at 60 °C. The solutions become clear after this process.
At different parameters, ZnO thin films were sprayed on heated glass substrates:
- We investigated undoped-ZnO thin films at temperatures ranging from 350 to 450°C with a 50°C step, at a pressure of 2 bar, and 11ml of precursor for each layer.
- We investigated undoped-ZnO thin films with varied deposition rates of 7, 11, and 13 ml at 2 bar pressure and 450°C glass substrate temperature.
- They investigated Zn-doped NiO thin films with different Ni content (0, 1, 5 and 6 percent), at 2 bar pressure and 450°C glass substrate temperature, using 10ml of precursor for each layer.

➢ **Nickel oxide**

The NiO solution was made by dissolving (0.05, 0.10, and 0.15 mol.l-1) from the commercial powder of Nickel nitrate hexahydrate Ni(NO3)2.6H2O in a solvent comprising equal quantities absolute H2O, then stabilizing the solution with drops of stabilized hydrochloric

acid HCl (97.7% purity). The combination solution was swirled and cooked for 3 hours at temperatures ranging from 25 to 50 degrees Celsius to produce a clear and transparent solution. NiO thin films of varied concentrations were sprayed on heated glass substrates at 450°C with 2 bar of solution pressure and 10 ml of precursor for each layer.

I.14.4. Deposition steps of thin films

The deposition of thin films using a solar-powered spray pyrolysis technique began with the preparation of the substrate, which was washed ultrasonically for five minutes in acetone, followed by deionized water for the same amount of time at room temperature, and finally dried; the substrate was then placed in its holder at the concentrator's focal point.

The precursor was prepared to the required specifications and placed in a bottle that was mounted on a movable support to control the distance between it and the substrates; the precursor was transformed into a droplet using air pressure, which was adjusted using the compressor's tap and pressure gauge.

The concentrator was rotated using a controlled tracking system, which is a mechanism that rotates the concentrator by tracking the sun in two axes using two pivot points. This sort of solar tracker generally has both horizontal and vertical axes.

When the concentrator was rotated to face the sun, the temperature of the substrate, as measured by the multimeter and thermocouple, rose to the target temperature, and the spray began to match the substrate temperature. Spraying is done sporadically because the temperature will be reduced after a period of spraying, allowing the solar heater to adjust the temperature; one of the advantages of this heat mode over electrical heating is the wait time, where the desired temperature is quickly returned, reducing the time of deposition.

I.15. Characterization techniques

In the following paragraphs we have exposed the different techniques used to characterize and measure the structural, electrical and optical properties.

I.15.1. Structural Characterization: X-ray Diffraction (XRD)

Generally, the study by X-ray diffraction allows us to specify the structure of the material (crystalline or amorphous). If the material is crystalline, we can determine other important parameters such as the directions of crystallographic growth of the deposited layers, the mesh parameters and the approximate size of the crystallites.

I.15.1.1. Principle of the XRD analysis

When a monochromatic X-ray beam is directed on a poly-crystalline material, it is partly reflected by the atomic planes of some crystals.

The diffraction will occur only in crystallized materials and when the Bragg relation is verified :

$$2d_{hkl} \sin\emptyset = n\lambda \qquad \text{Equation 1}$$

dhkl : is the inter-reticular distance, that is to say distance between two crystallographic planes,

θ: the angle of incidence and thus the angle of reflection with respect to these planes,

λ : the wavelength of the incident X-ray photons,

n : the order of diffraction (integer).

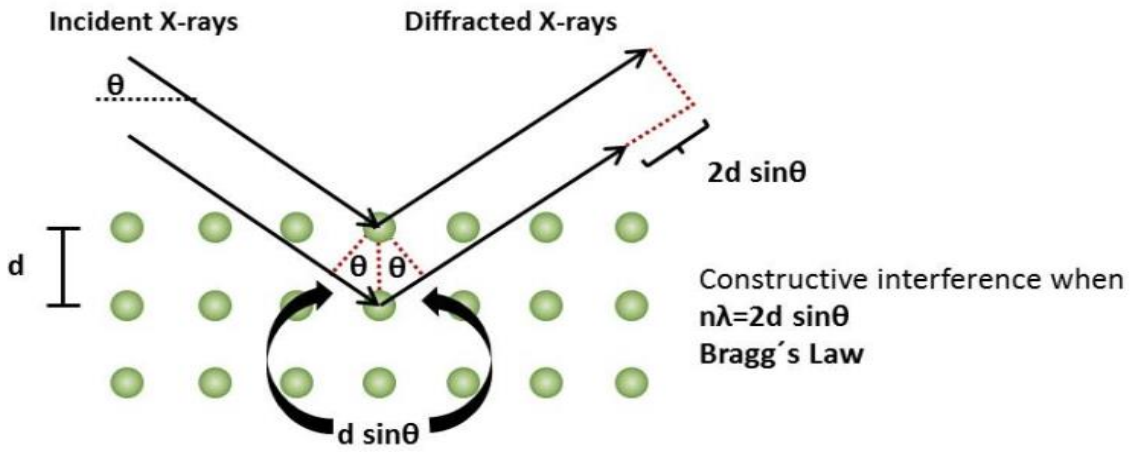

Figure 23 : *Schematic representation of Bragg equation* [44]

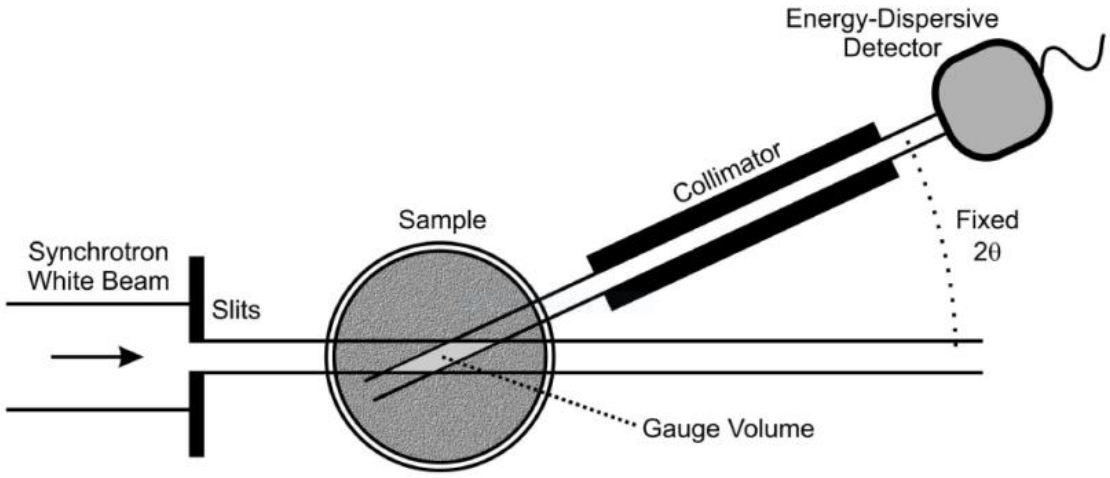

Figure **24 :** *Diagrammatic representation of the energy dispersive diffraction (EDD) method. The energy discriminating detector at fixed scattering angle determines the wavelength of each detected photon and thus the interplanar spacing d of the diffracting lattice planes* [24].

In the diffractometer, X-rays were produced from a source of CuKα radiation, having a wavelength equal to 1.540593 Å.

I.15.1.2. Determination of crystal parameters

To calculate the crystalline parameter (lattice parameter "a") for the thin films, we used the interplanetary distance (hkl) relationship and the crystallographic modulus
Crystal parameter [45]:

$$\frac{1}{d_{hkl}^2} = \frac{h^2+hk+k^2}{a^2}$$ Equation 2

I.15.1.3. Determination of crystallite size

For the estimation of the crystallite size of different samples from the diffraction spectra, we used diffraction spectra, we used the formula of Scherrer [46,32] :

$$D = \frac{0.9\lambda}{\beta \cos\theta}$$ Equation 3

Where the parameters:
D : the size of the crystallites,
ʎ : the wavelength of the X-ray beam,
β : the width at half height of the diffraction line, expressed in radian
θ : the diffraction angle.

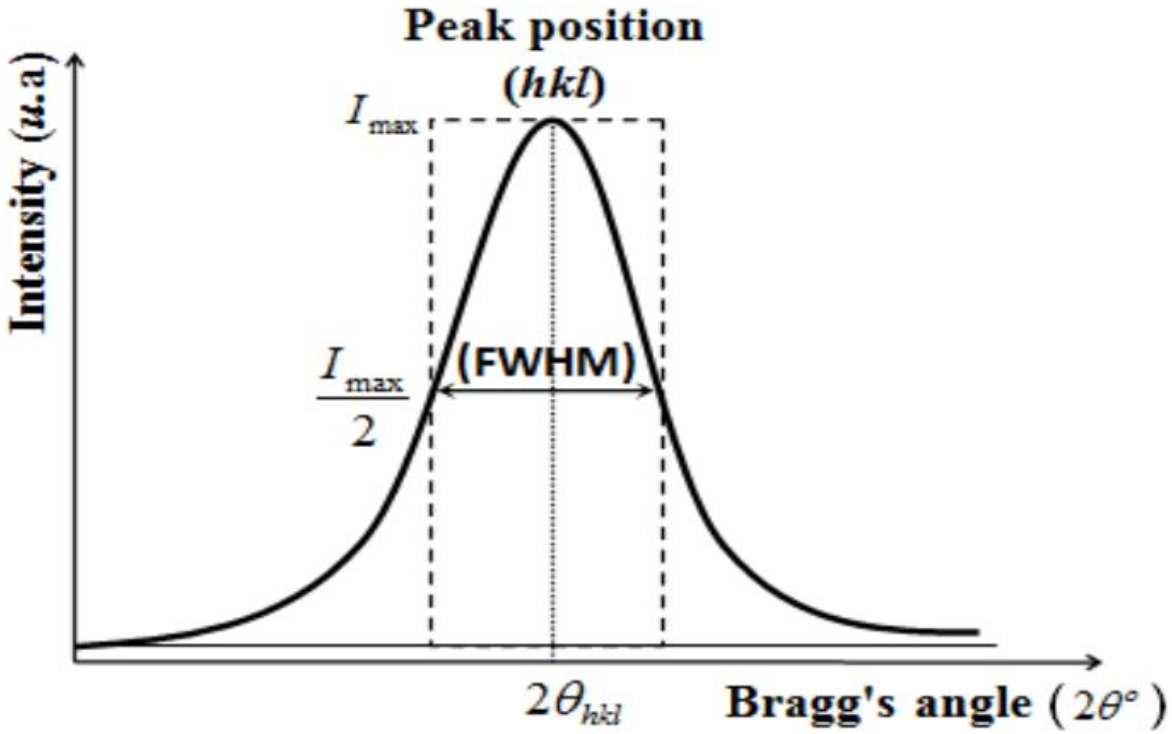

Figure 25 *: Full width at half maximum (FWHM) of a peak.*

I.15.2. Optical characterization

Optical methods allow to characterize a large number of parameters. They have the advantage over electrical methods of being non-destructive and do not require the reaction, of ohmic contacts.

We distinguish two types of optical methods:

- The methods that study the optical response of the material to an excitation such as photo and cathodo-luminescence.
- Methods that analyze the optical properties of the material such as; transmittance and reflectance measurements and ellipsometry measurements. These spectroscopic measurements can determine the optical refractive index, the thickness of the material and the optical gap.

I.15.2.1. Spectroscopie UV-visible

In this work, some parameters of the optical properties of thin films (band gap width, Urbach energy) have been determined by exploiting curves representing the variation of transmittance as a function of wavelength in the UV-visible range.Indeed, we used a UV-Visible spectrophotometer (SHUMATZU 1800) [it is a double beam spectrometry, one for the reference (glass) and the other for our sample (the thin layer of nickel oxide + Zinc oxide + glass)] and whose spectral range extends from the UV-Visible (λ=300-900 nm). The principle of operation of this device is shown in Figure 26

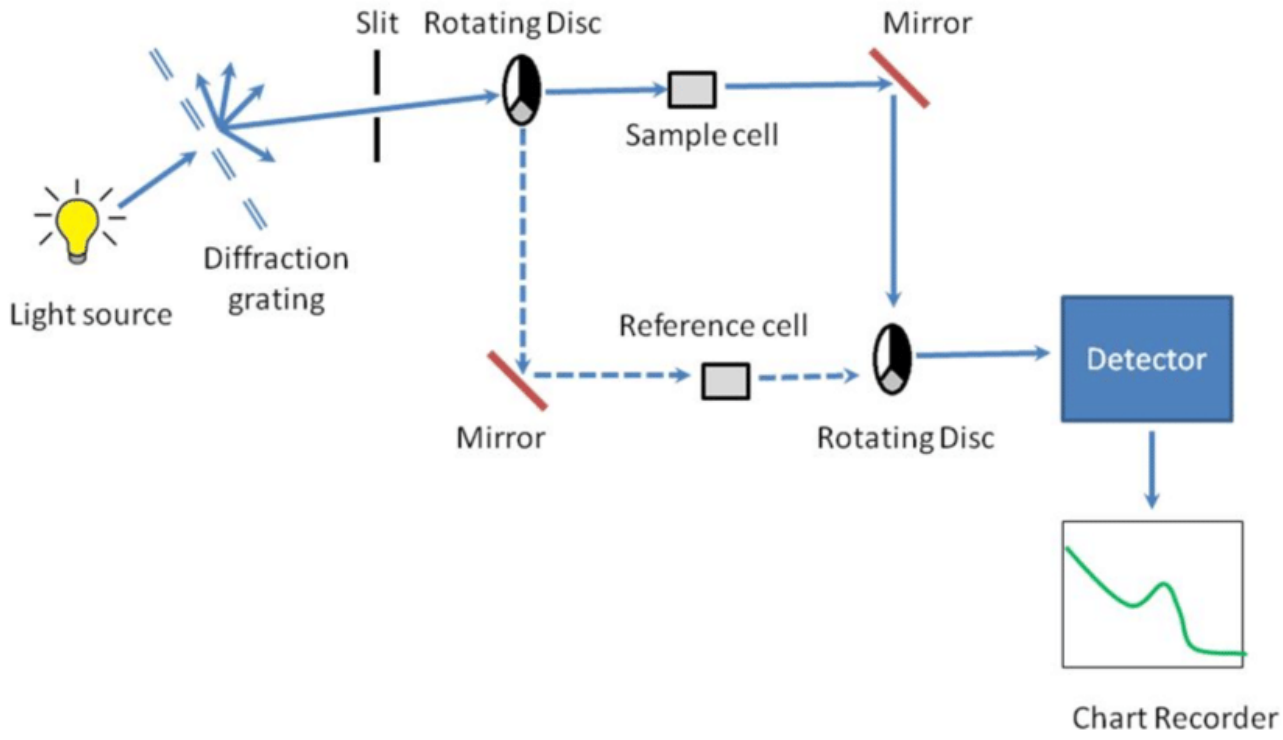

Figure 26 : *Schematic representation of the UV-Visible spectrophotometer* [47]

Figure 27 : *Experimental UV-visible spectroscopy device **UV-1800** used*

I.15.2.2. Thickness measurement of thin films

The thickness of the thin films was determined from transmittance spectra, using a "Fit" software [48] that allows to vary a number of parameters, such as thickness, refractive index and optical gap and to use the least squares method to fit a simulated transmittance curve to the measured one. Figure 28 is an example of the determination of the thickness of the thin layer

(a) Serial Number	(G5S2)	(G2S2)	(G1S1)	(G3S5)
Growth Time (min.)	5	2	1	3
Shutting Time (min.)	2	2	1	5
Thickness (nm)	570	580	570	570

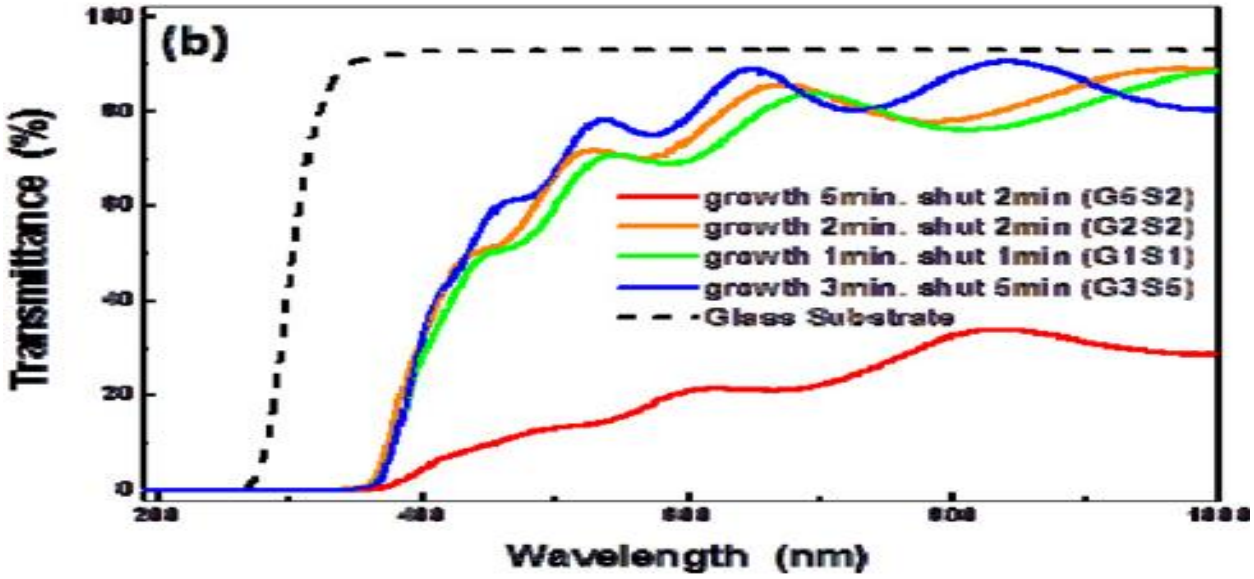

Figure 28 : *Calculation of the thickness from transmittance spectrum (Layer developed at 2.5 min)* [49]

It should be noted that we can calculate the thickness of a sample by the method of bangs (layer deposited at 5 min). This technique is based on the knowledge of inter-fringes in the transmission spectra [50].

I.15.2.3. Determination of the optical gap

The expression for the absorption coefficient of absorption (α) for the optical gap (Eg) and the energy (hν) for photons is written in the form (Tauc's equation) [51]:

$$(\alpha h\nu)^2 = A(h\nu - E_g) \qquad \text{Equation 4}$$

Where: A is a constant, Eg is the band gap width (or optical gap expressed in eV) and *h*υ is the energy of a photon in eV $(\mathbf{hv(ev)} = \frac{\mathbf{hc}}{\lambda} = \frac{\mathbf{12400}}{\lambda(\mathbf{Å})})$

The value of the optical gap is determined by extrapolating to $\alpha^2 = 0$ the line giving $(\alpha h\upsilon)^2$as a function of *h*υ (Figure 29).

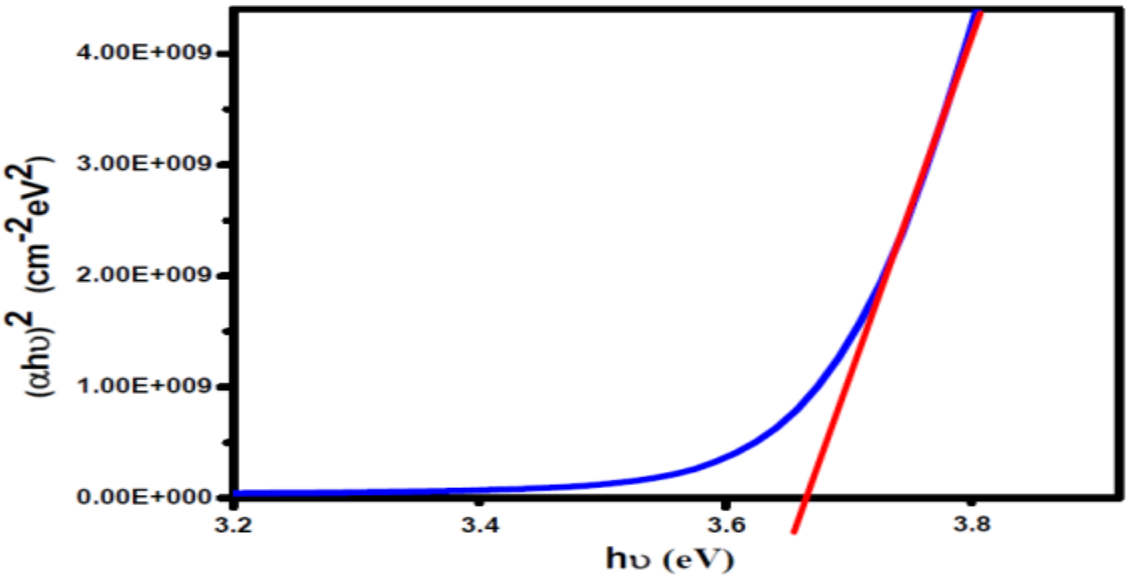

Figure 29 : *Determination of the energy gap for a NiO thin film* [51]

I.15.2.4. Determination of the Urbach energy

In the field of study of optical properties, we calculated the Urbach energy (Eu) to determine the state of disorder of the material. Indeed, the absorption coefficient, according to the law of Urbach, is given by the relation [52,53]:

$$\boldsymbol{\alpha = \alpha_0 EXP\left(\frac{h\upsilon}{E_u}\right)} \qquad \text{Equation 5}$$

We can also write:

$$Ln\alpha = Ln\alpha_0 + \frac{h\upsilon}{E_u} \qquad \text{Equation 6}$$

Therefore, the value of the Eu parameter is determined from plotting lnα versus *h*υ (Figure 30).

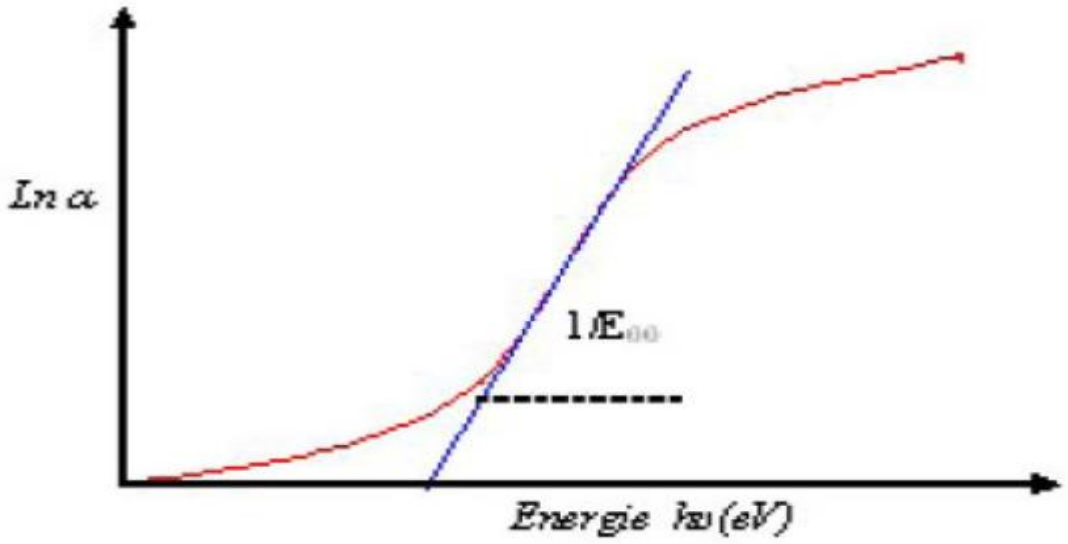

Figure 30 : *Example of the determination of the Urbach energy from the variation of ln α as a function of hν for a thin film* [52]

I.15.3. Electrical characterization

In order to know directly the surface resistance Rs, we have used a four-point device, model KEITHELY SRM 2400 device, model KEITHELY SRM 2400 figure 31. The probe is made of four aligned and regularly spaced contacts aligned and regularly spaced, figure 32. A

source provides a current I flowing through the outer terminals. The voltage U is measured across the two inner tips. The use of four contacts instead of two, as in a classical resistance measurement the resistance of the pins and to measure only the resistance of the sample. of the sample. When the distance "a" between the terminals is much greater than the thickness of the thin film, the lateral dimensions can be considered as infinite. In this case, a two-dimensional model of conduction is considered and gives :

$$\frac{U}{I} = K\frac{\rho}{d} \qquad \text{Equation 7}$$

Where: ρ: the resistivity of the layer and d: the thickness.

The ratio characterizing the layer is noted $R_s$and is expressed in Ω. At a ready coefficient K, R is the ratio between the voltage U and the current I. Considering a cylindrical propagation of the field lines in the thin layer, the in the thin layer, the coefficient K is (ln2/π).

From the relation (III.7), we have the formula (III.8) to deduce the resistivity of the four point measurement knowing the thickness d of the thin layer:

$$\rho = \left(\frac{\pi}{ln2}\frac{U}{I}\right)d = R_s d \qquad \text{Equation 8}$$

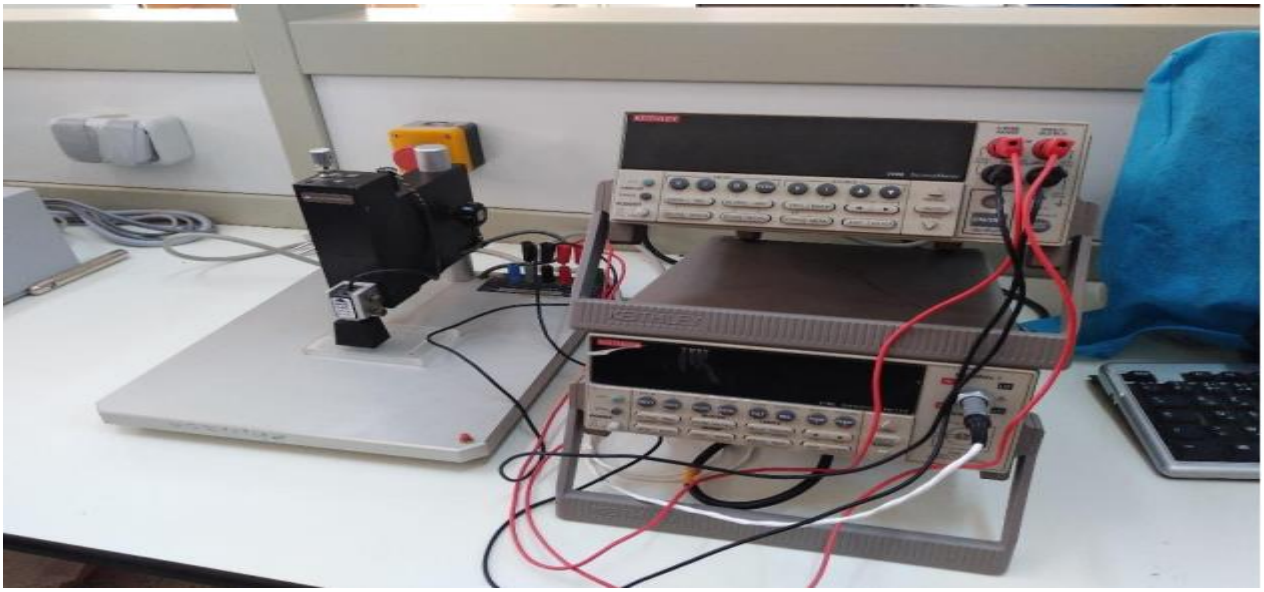

Figure 31 : *Experimental setup of device of the Four-Probe Method used (KEITHLEY 2400)*

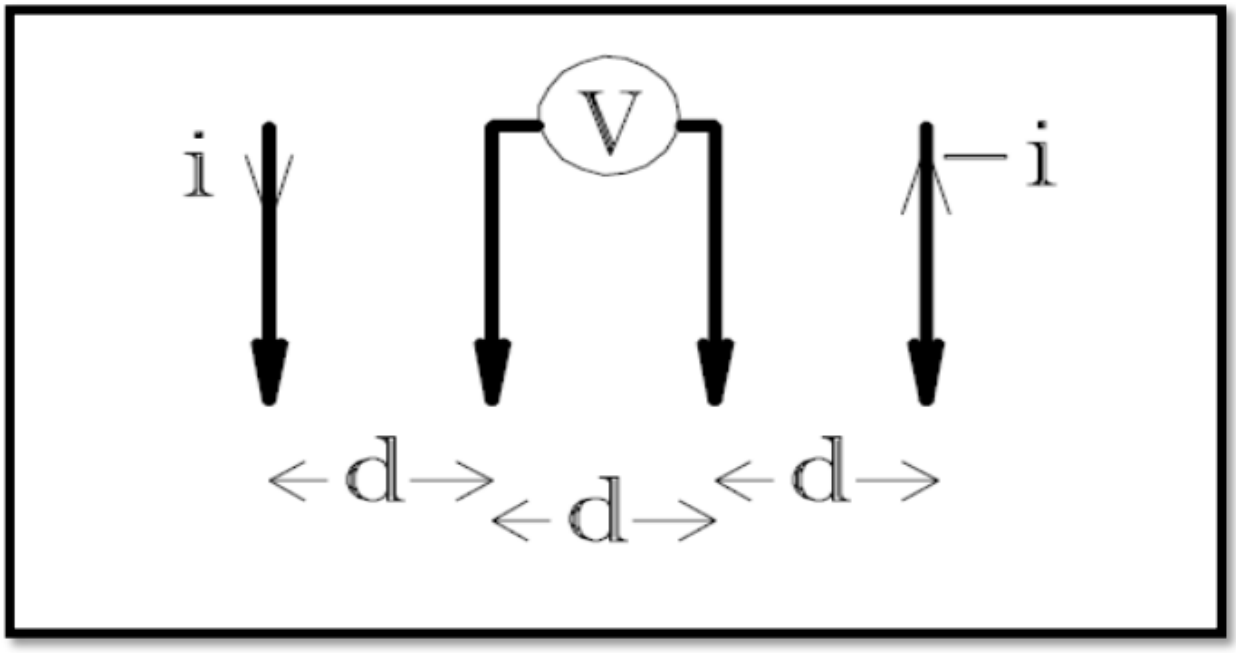

Figure ***32 :*** *K value (special case)*

I.16. Conclusion

In this chapter, we thoroughly discussed the experimental setup of a handmade solar spray pyrolysis system, including the concentrator, air compressor, atomizer, receiver (substrate holder), multimeter, and thermocouple. The concentrator's heating of the substrates was then shown. Following that, we reviewed experimental specifics, including the preparation technique for all forms of oxide under various circumstances, as well as how to prepare the substrates. We included the techniques we utilized to characterize our thin films at the conclusion of the chapter, including X-ray diffraction (DRX), UV Visible spectroscopy, and the four-point approach.

Chapter IV : Results and Discussion of Obtained Zn-Doped NiO Thin Films

I.17. Introduction

The major experiment results finding of deposition of Zn-doped NiO thin films at various Zn contents with the use of spray pyrolysis technique and solar energy as a source of heat are presented and discussed in this chapter.

I.18. Characterizations of prepared Zn-doped NiO thin films

We deposited a serie of Zn-doped NiO thin films on glass substrates heated by a solar system using spray pyrolysis, and we will study the dopant effect on structural,optical and electrical proproties of obtained layers.

I.18.1. The crystalline structure of Zn-doped NiO thin films

In figure 33 the X-ray diffraction spectra results of the crystalline structure of Zn-doped NiO thin films are shown.

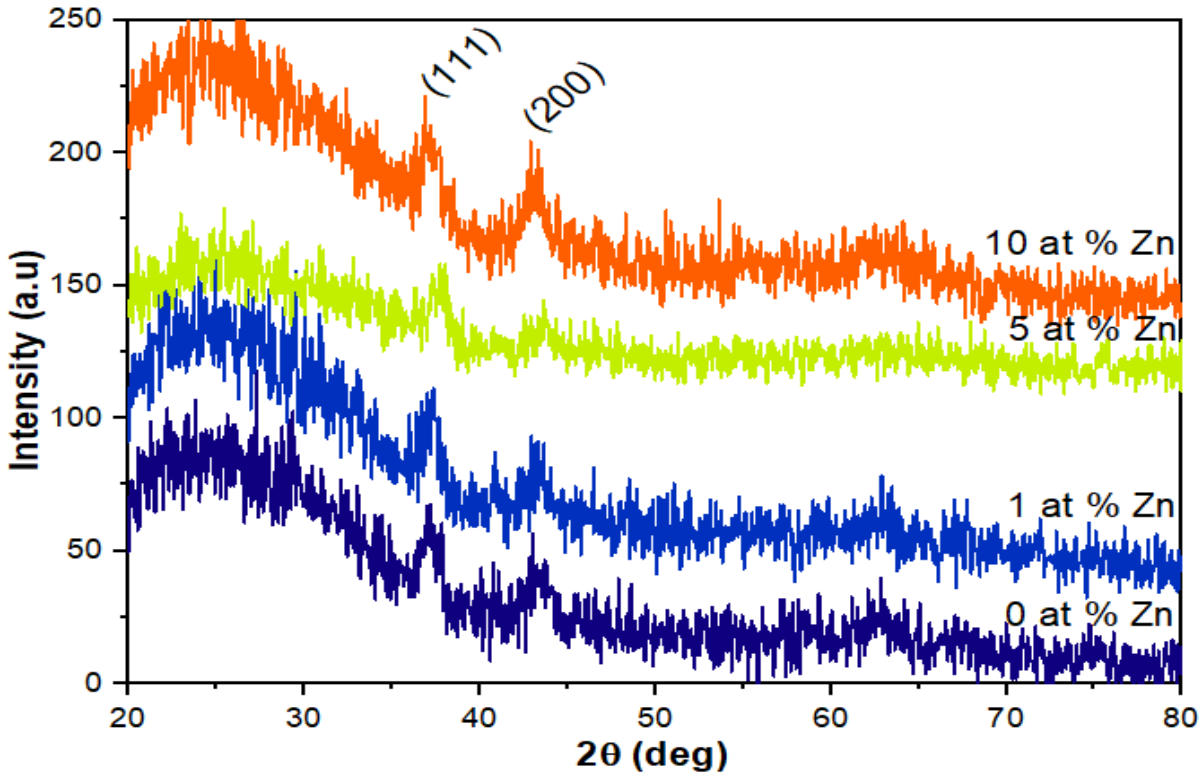

Figure **33 :***The XRD spectra of Zn- doped NiO thin films with various Zn contents*

It can be observed that all the patterns exhibit two diffraction peaks around 2θ ~ 37,26° corresponding (111), and 2θ ~ 43.29 corresponding (200) diffraction peaks of the NiO crystal structure. The diffraction peak of (111) has the highest intensity. When the Zn content increases from 0 at% Zn to 10 at% Zn, the intensity of peaks increases..

The measurement of the crystallite size according to the Scherrer equation represents the deep structure information of Zn-doped NiO thin films.

The variation of the crystallite size of the (111) diffraction peak as a function of deposition Zn content is shown in Figure 34.

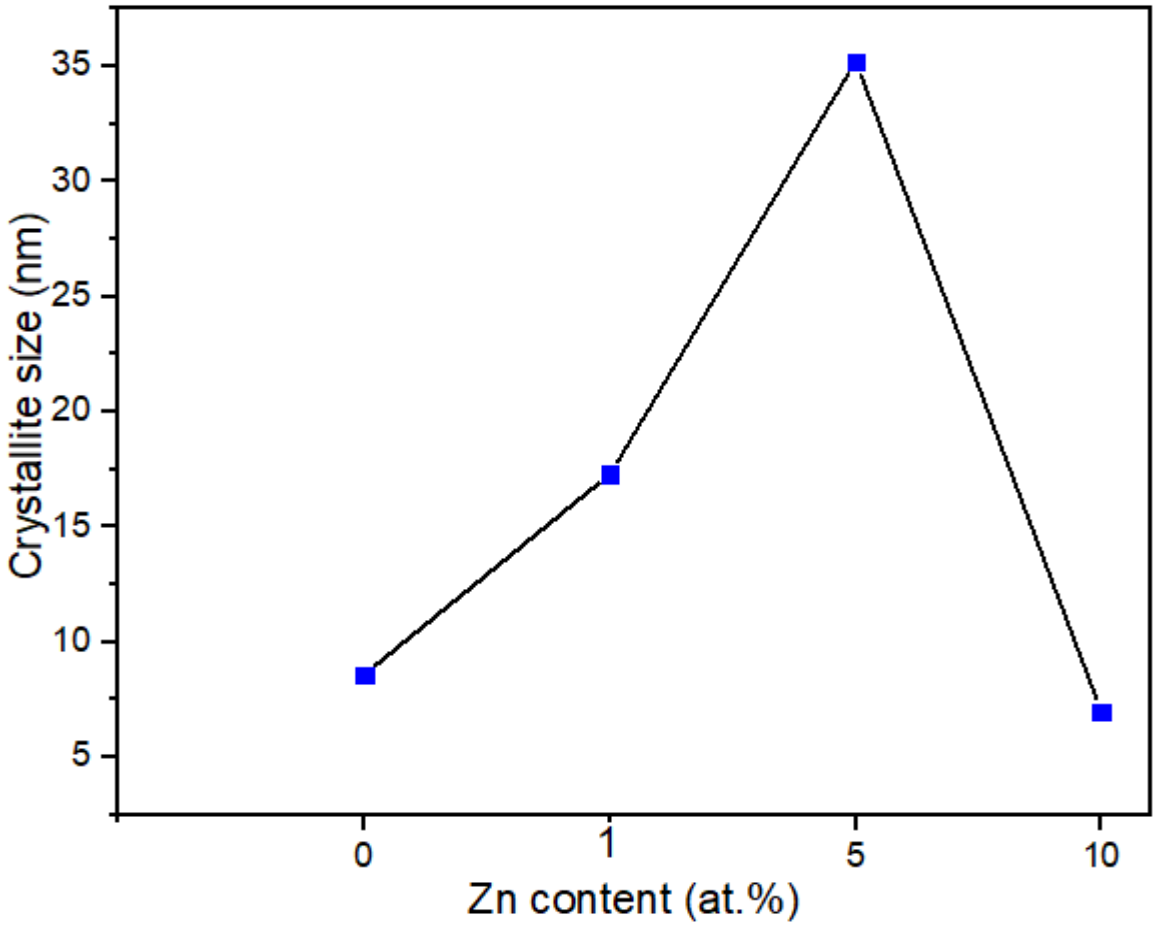

Figure **34 :***The variation of crystallite size of (111) plane in Zn-doped NiO thin films versus Zn content*

Figure 34 shows that by increasing Zn contents from 0 to 5 at %, the crystallite size increase greatly from 8.55 to 35 nm. Then more than 5 at% to 10 at % the crystallite size decrease.

As for the figure 35, it shows the variation of the lattice strain from the diffraction peak (111) as a function of the zinc dopants levels

This experimental results of lattice strain of Zn-doped NiO thin films decrease greatly with the increase of doping level from 1,25 to 0,4 % corresponding 0 at% to 5 at% ,after that the lattice strain increase until reach the value 1,55 corresponding 10 at % of zinc content .

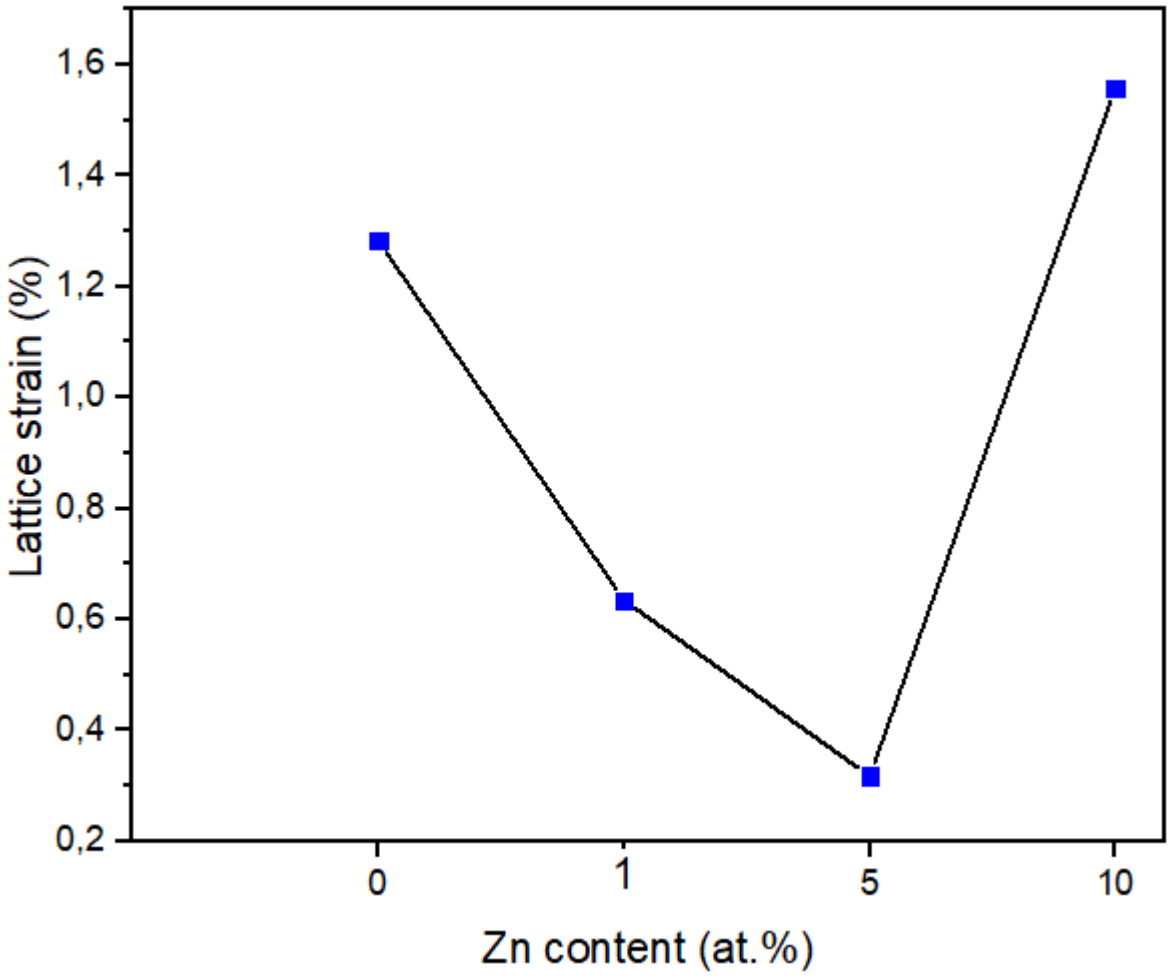

Figure **35 :***The variation of lattice strain of (111) plane in Zn-doped NiO thin films versus Zn content.*

I.18.2. The optical properties of Zn-doped NiO thin films

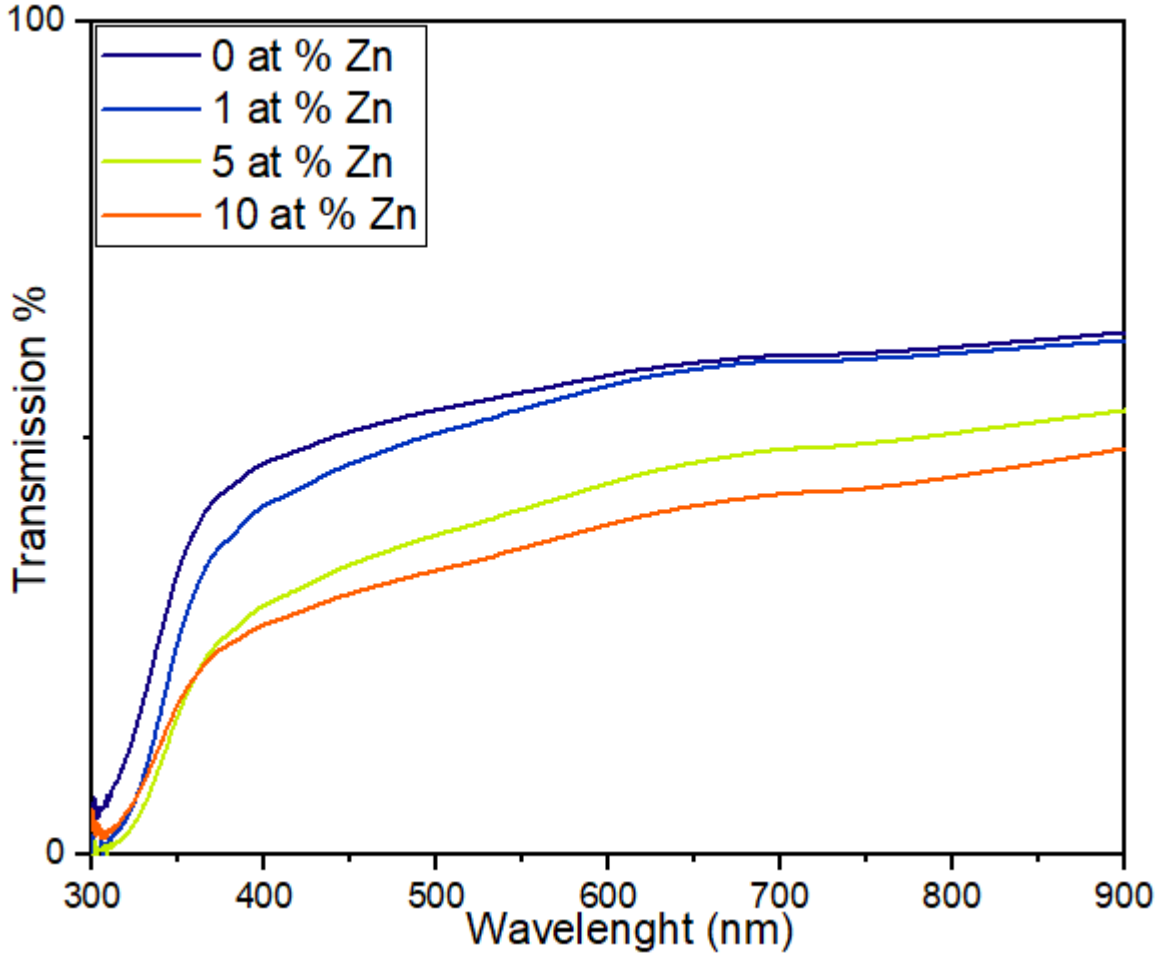

Figure **36 :** *Transmission spectra of Zn-doped NiO thin films as a function of Zn content*

Figure 36 represents The optical transmission of Zn-doped NiO layers at different Zn contents. As the Zn content increase from 0 at % to 10 at % , the transmission was decreased, where this decrease are explained by the increase in the film thickness. But these thin layers have a medium transmission with comparing by other NiO thin films. The region of low transmittance was found between λ = 330 to 380 nm, in this region, the absorbance increased because of the migration and the excitation of the electrons from the valence to the conduction band. The vector which has directly effect in the electrical conductivity of the thin films is the optical bandgap energy , which based on optical transmission. It was determined by the extrapolation method of the curve at $\alpha = 0$, which represented to the drawn of the $(\alpha h\upsilon)^2$ as a function of hυ (see Figure 37)

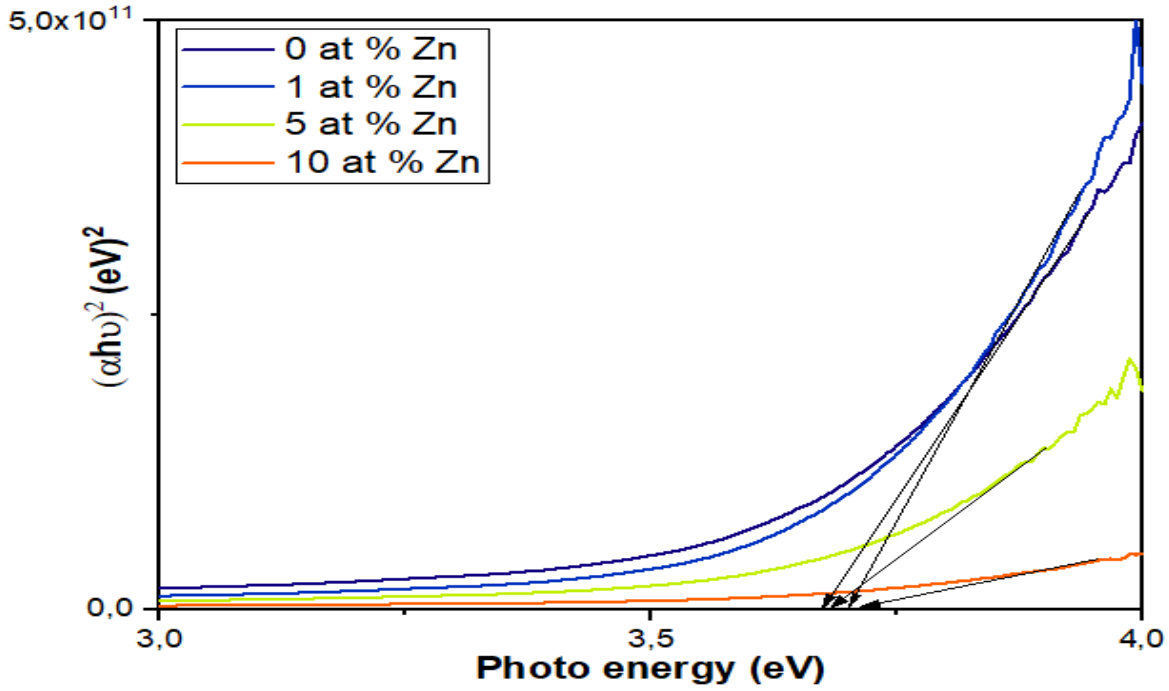

Figure 37 :*The variation of* $(\alpha h\nu)^2$ *as a function of* $(h\nu)$ *for each films thickness for calculate optical energy.for Zn-doped NiO thin films versus Zn content.*

On the other hand, the urbach energy of prepared Zn-doped NiO this films wich represents the disorder in the layers was calculated by the following expression

$$\alpha = \alpha_0 \exp^{\left(\frac{h\upsilon}{E_u}\right)}$$

where α_0 a constant hυ is the photon energy and E_u is the Urbach energy,
in Table 04 ,the values of optical bond gap energy and urbach energy are represented .
Figure 38 shows the drawn of Lnα as a function of photon energy hυ for deducing the Urbach energy.

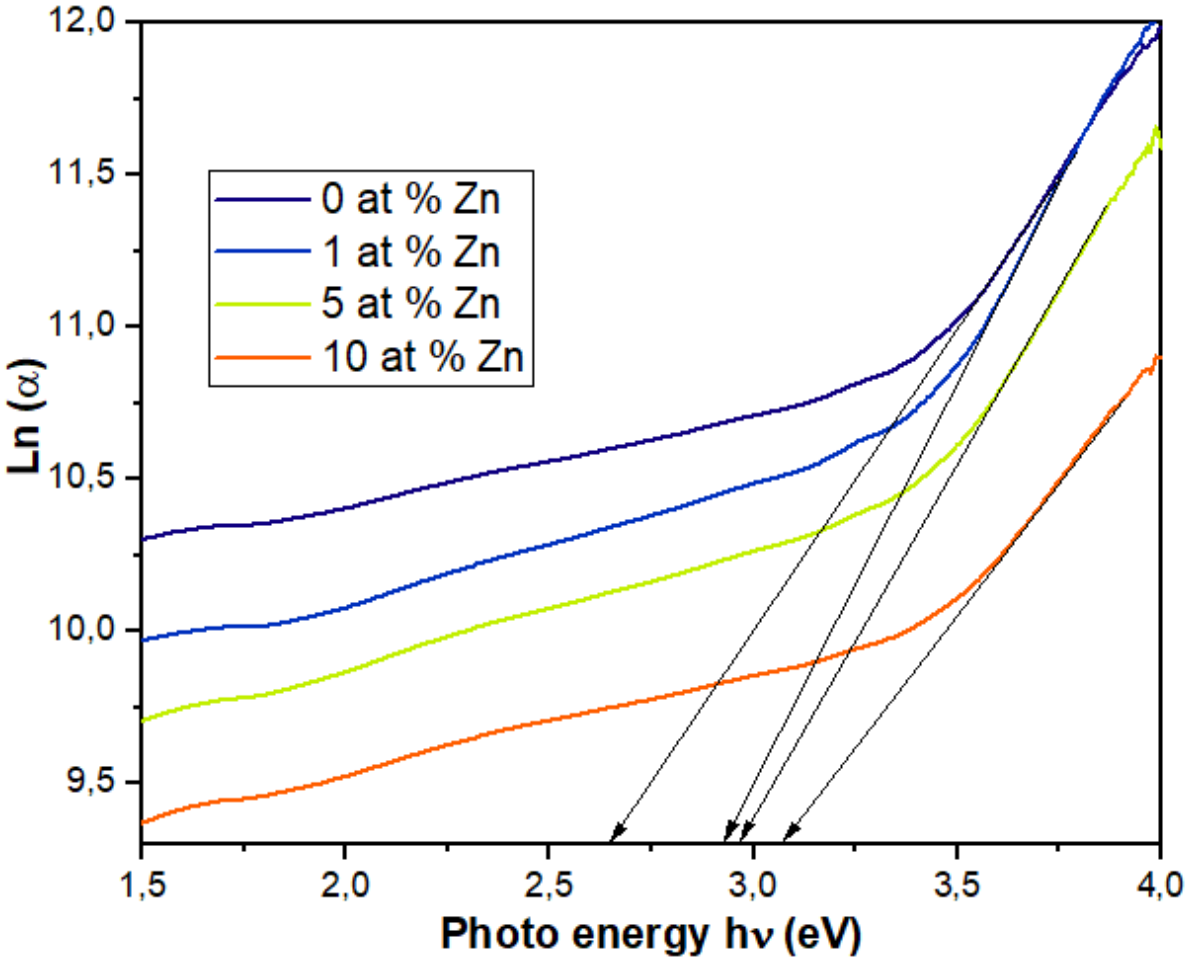

Figure **38 :***The variation of(lnα) versus(hν)for estimated Urbach energy for Zn-doped NiO thin films versus Zn content*.

Figure 39 demonstrates how the optical gap energy and Urbach energy of Zn-doped NiO thin films vary depending on the Zn content.

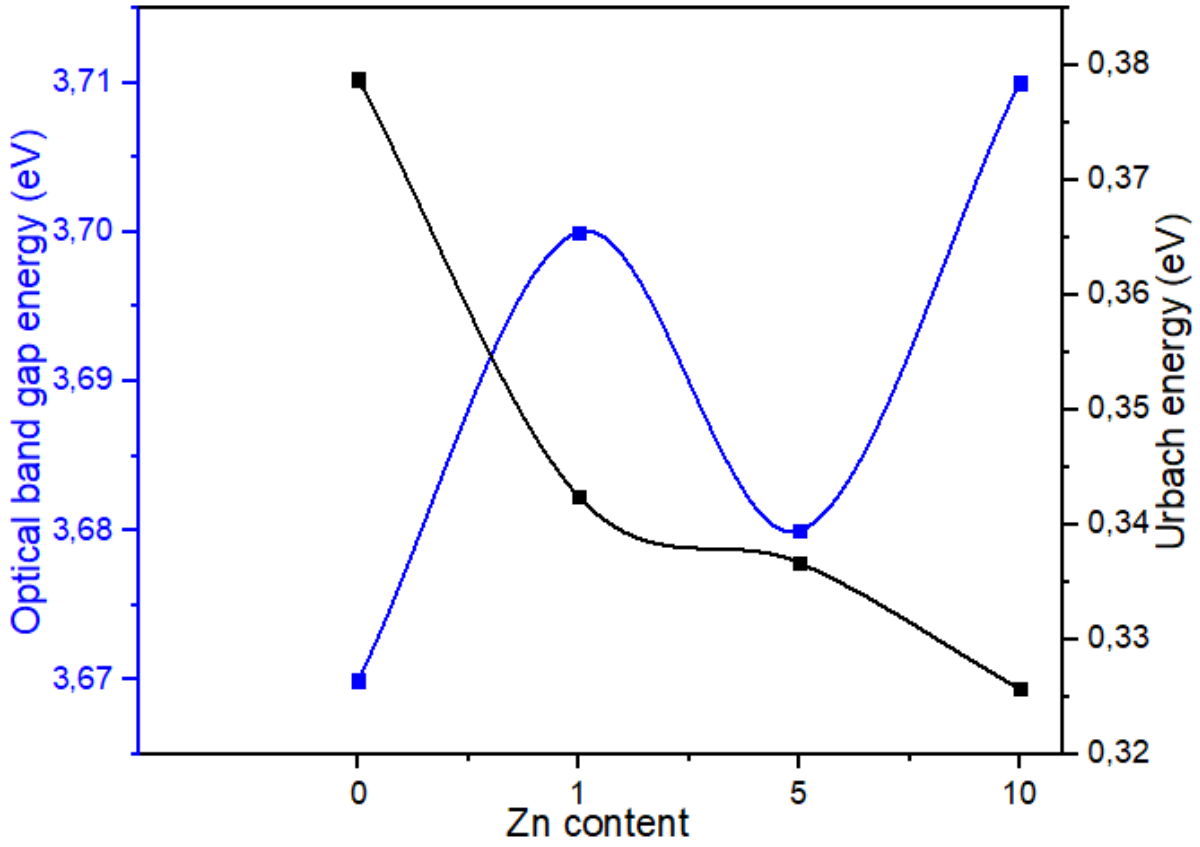

Figure **39 :***The variation of optical band gap Eg and Urbach energy Eu of Zn-doped NiO thin films versus Zn content.*

Because of the conduction band and valence band, the change is inverse: as the doped level of Zn increases, the optical band gap energy increases until the value of 3,7 ev corresponding 1at % Zn then decreases at 5at %Zn after that increase to reach 3,71 ev . The

growth was influenced by the crystallite size increase (see Figure 35 , 36). However , Urbach energy increasing with the increase of Zn content ti reach 0,3257ev, indicating that the Zn-doped NiO thin film prepared at 10% has less disorder and fewer defects, which could be attributed to a decrease in crystallite boundary for an increase in deposition Zn content;

The Urbach tail energy (Eu) is calculated using the equation. The values of Eg and Eu in table IV.1 are the results of this calculation.

Table IV.1 : *Recapitulating measured values of band gap energy Eg Urbach energy Eu for Zn-doped NiO thin films as a function of deposition rate.*

deposition rate (%)	Eg **(eV)**	Eu **(eV)**
0	3.67	0,378788
1	3.7	0,342466
5	3.68	0,3367
10	3.71	0,325733

I.18.3. The electrical resistivity of Zn-doped NiO thin films

The electrical resistivity of Zn-doped NiO thin films varies as a function of doped lavel of Zn, as shown in Figure [40]. As a consequence, when the deposition Zn content was raised from 0% to 1%, the electrical resistance increased from 2.5×10^{-4} to $1.4 \times 10^{-3}(Ohm.cm)^{-1}$, then declined to up to $2.0 \times 10^{-4}(Ohm.cm)^{-1}$for 5%. After that, it rises to $2.3 \times 10^{-4}(Ohm.cm)^{-1}$for 10%. The rise in resistivity can be explained by the crystallite size increasing (see Figure 35 , 36).

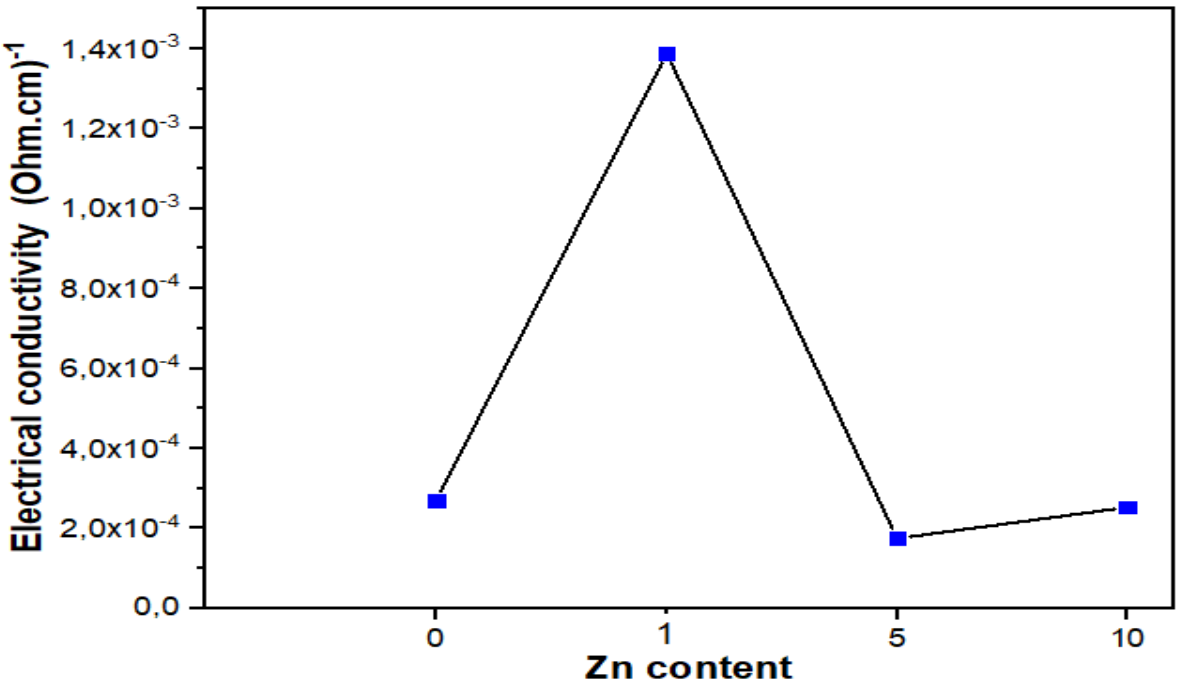

Figure 40 **:** *The variation of electrical conductivity and film thickness of Zn-doped NiO thin films versus Zn content.*

I.19. Conclusion

In the fourth chapter, we employed spray pyrolysis and solar heating to make Zn-doped NiO thin films with varied Zn content, and then investigated the structural, optical, and electrical characteristics of the samples created. All of the samples possessed a polycrystalline structure, according to the XRD patterns. (111) and (200) have the largest diffraction peaks. In the Zn-doped NiO samples, he doping. The transmittance spectra revealed an average optical transmission of roughly 60 percent in the visible area for all samples. It lowers as the deposition period and Zn concentration of the substrate of Zn-doped NiO thin layer increases. The gap energy reduces when all of the deposition parameters are changed, and the electrical conductivity increases as the deposition rate is increased.

General conclusion

General conclusion

We began exploring the structure, characteristics, and potential energy that we may obtain from the sun in this 1er chapter, as well as the dimensions, effects, and various equipment necessary for a proper examination of solar energy, as well as the possible methods for producing thin films.

After, We talked about thin films in the second chapter. We also looked at some of the applications for this layer, as well as a comprehensive examination of zinc and nickel oxide to show their structural, optical, and electrical characteristics. The chapter came to a close with a description of thin-film preparation processes and a discussion of the spray change method.

The experimental setup of the hand-made solar spray pyrolysis system, comprising the condenser, air compressor, filter, receiver (pillar holder), multimeter, and thermocouple, was extensively covered in the third chapter. After that, the heating of the substrates was shown. The experimental parameters were then reviewed, which included the preparation process for all forms of the oxide under various circumstances as well as how to prepare the substrates. At the end of the chapter, we listed the techniques we utilized to characterize our thin films, including X-ray diffraction (DRX), UV spectroscopy, and the four-point approach.

In the fourth chapter, we employed spray pyrolysis and solar heating to make Zn-doped NiO thin films with varied Zn content, and then investigated the structural, optical, and electrical characteristics of the samples created. All of the samples possessed a polycrystalline structure, according to the XRD patterns. (111) and (200) have the largest diffraction peaks.

The transmittance spectra indicated an average optical transmission of roughly 60 percent. It decreased with the increase of zinc content. the electrical conductivity rises as the Zn content rises.

the future studies which we suggest are to use other oxides with the improving of depositions conditions to obtain better results.

References

References

[01] Y. Benkhetta, "L'effet du débit de la solution sur les propriétés des couches minces d'oxyde de zinc (ZnO) déposées par spray ultrasonique," 2013.

[02] L. Smaoun, C. Bellagh, and N. Ait Ahmed, "Électrodéposition des couches minces de l'oxyde de nickel et étude de leur activité électro catalytique vis-à-vis de l'oxydation du Méthanol et du Propanol," University of Abderrahmane Mira-Bejaia, 2016.

[03] Hancock, N, Solar Water Distillation. Safe Drinking Water Foundation. https://www.safewater.org/fact-sheets-1/2016/12/8/solar-water-distillation. (2019, February 22).

[04] Solar Drying. Solar Drying - an overview | ScienceDirect Topics. (n.d.). https://www.sciencedirect.com/topics/engineering/solar-drying, Renewable and Sustainable Energy Reviews, 2018.

[05] Jump up to: 4.0 4.1 What You Need to Know About Energy, Our Energy Sources: The Sun [Online]. Available: http://needtoknow.nas.edu/energy/energy-sources/the-sun/,July 31, 2015.

[06] ITACA, The Sun as a Source of Energy [Online]. Available: http://www.itacanet.org/thesun-as-a-source-of-energy/part-2-solar-energy-reaching-the-earths-surface/, (August 4, 2015).

[07]Renewable and Sustainable Energy Reviews 68, 541-562, 2017 Available: https://doi.org/10.1016/j.rser.2016.09.104.

*[08] https://miro.medium.com/max/900/1*lb_gXj8OO_iu91gMhB7jxw.jpeg*

[09] Solar Water Distillation System Available: https://mechanical.srpec.org.in/files/Project/2013/6.pdf.

[10] https://cpimg.tistatic.com/05445247/b/4/Solar-Distillation-Plant-w300.jpg.

[11] VS Korpale, DH Kokate, SP Deshmukh Energy Procedia 90, 518-524, 2016Available: https://doi.org/10.1016/j.egypro.2016.11.219.

[12] Philipp Haueter, T Seitz, Aldo Steinfeld Journal of Solar Energy Engineering 121 (1), 1999Available: https://www.osti.gov/biblio/330503/.

[13] EIA. (August 18, 2015). Solar Thermal Power Plants [Online]. Available: http://www.eia.gov/Energyexplained/?page=solar_thermal_power_plants.

[14] Article in Instrumentation Mesure Metrologie • November 2020 DOI:

[15].18280/i2m.190507Available:https://www.researchgate.net/publication/3465035/.

[16]https://molecularworkbench.blogspot.com/2017/07/modeling-linear-fresnel-reflectors-in.html?m=&/.

[17] Wikimedia Commons. (April 5, 2018). Solar Stirline Engine [Online]. Available: https://commons.wikimedia.org/wiki/File:SolarStirling_Engine.jpg.

[18] Article in Energy Conversion and Management • August 2016 Available: https://www.researchgate.net/publication/305811492/.

[19] Parabolic solar cooker designs 23 December 2021 Available: https://solarcooking.fandom.com/wiki/Category:Parabolic_solar_cooker_designs/.

[20] Maaoui, Bedreddine. Procédé de dépôt de matériaux nanacomposites a l'aide d'énergie solaire. Diss. University of Eloued 2021 جامعة الوادي،

[21]https://encryptedtbn0.gstatic.com/images?q=tbn:ANd9GcSMWf1GDSG3pVXW04qJTDhHlT0e11Y6c2ofSg&usqp=CAU.

[22] AOUN, Y., Conception et développement d'un four solaire pour l'élaboration des oxydes Métalliques-caractérisation des oxydes. 2016, Université Mohamed Khider-Biskra.

[23] Shi-Ming, Z., et al., Atomic simulation of SiyHx structure configuration in a-Si: H thin films.ACTA PHYSICA SINICA, 2020. 69(7

[24] "L'effet de la molarité de nickel sur les propriétés des couches minces d'oxyde de nickel NiO élaborées par la technique de spray pyrolyse alimentée par énergie solaire." (2019).

[25] L. Tomasini, Les traitements de surface sous vide, (SOLLAC, Groupe Usinor), La Revue de Métallurgie - CIT Avril (2001).

[26] H. Benzarouk, Synthèse d'un oxyde transparent conducteur (OTC) par pulvérisation chimique (ZnO, NiO), Mémoire de magister, université badji mokhtar, Annab.

[27] Berrouis Soumia, Bensefira Dallal. "Elaboration et caractérisation de couche mince NiO: Co." 2019

[28] L. Smaoun, C. Bellagh, Électrodéposition des Couches Minces de l'oxyde de Nickel et étude de leur activité électro catalytique vis-à-vis de l'oxydation du Méthanol et du Propanol, Mémoire de Master, Université A. MIRA, Bejaïa, 2015

[29] WebElements, Nickel oxide. May 2021.

[30] Saraç, B.E., Structural and optoelectronic properties of sol-gel derived nickel oxide thin films 2017, MIDDLE EAST TECHNICAL UNIVERSITY.

[31] مذكرة Fe(,) المطعم بالحديد NiO( )ط. مصباحي ،ع. دقة ،تحديد بعض خصائص اغشية اكسيد النيكل
مـــاستر أكـــاديمي، جـــامعة الشهيد حمه لخضر، الوادي

[32] Benramache, Said. Elaboration et caractérisation des couches minces de ZnO dopées cobalt et indium. Diss. Université Mohamed Khider-Biskra, 2012

*[33] Rahmane, Saâd. LABORATION ET CARACTERISATION DE COUCHES MINCES PAR SPRAY PYROLYSE ET PULVERISATION MAGNETRON. Diss. Université Mohamed Khider Biskra, 2008.**

[34] Bedia, Asma. "Synthèse et caractérisation des nanostructures d'oxyde de zinc (ZnO) pour des dispositifs a applications biomédicales." Thèses De Doctorat, UniversiteUniversite (2015

[35] H.J.Michel,H.Leiste,K.D.Scheibaum,J.Halbritter. Adsorbates and their effects on gas sensing properties of sputtered SnO2 films, Appl.Surf.Sci.126 (1998): 57–64.

[36] R.Ayouchi, D.Leinen,F.Martin,M .Gabas,E.Dalchiele,J.R.Ramos-Barrado, Preparation and characterization of transparent ZnO thin films obtained by spray pyrolysis, Thim Solid Film. 42 (2003): 68–77.

[37] Shi, F., Introductory Chapter: Basic Theory of Magnetron Sputtering, in Magnetron Sputtering. 2018, IntechOpen.

[38] A.Antony, K.V.Mirali, R.Manoj, M.K.Jayaraj, The effect of the pH value on the growth and properties of chemical-bath-deposited ZnS thin films Mater.Chem.Phys.90 (2005): 106 -110.

[39] J. Garnier, Elaboration de couches minces d'oxydes transparents et conducteurs par spray CVD assiste par radiation infrarouge pour applications photovoltaïques, Thèse de doctorat, ENAM-0030 (2009).

[40] OTHMANE, M., Synthesis and characterization of Zinc Oxide (ZnO) Thin films deposited by spray pyrolysis for applying: electronics and photonics. 2018, UNIVERSITE MOHAMED KHIDER BISKRA

[41] Maache, Mostefa. Dépot et caracterisation de couches minces de ZnO par spray pyrolyse. Diss. Universite Mohamed Khider-BISKRA, 2005.

[42] ACHOUAK, HEMEIR Wassila-KHAMOULI. MÉMOIRE DE MASTER`.2019.

[43] https://www.researchgate.net/figure/Thin-film-process-steps-For-all-steps-process-monitoring-is-valuable-and_fig27_27560704

[44] Eby, G.N., 2004, Principles of Environmental Geochemistry. Brooks/Cole-Thomson Learning, p. 212-214.

[45] H.Benzarouk, Synthèse d'un oxyde transparent conducteur (OTC) par pulvérisation chimique (ZnO, NiO), Mémoire de magister, Université d'Annaba (Algérie), (2008).

[46] H.Nanto, T.Minami, S.Takata, Phys. Stat. Sol. A. 1981, 65, K 131.

[47] https://www.researchgate.net/figure/Schematic-diagram-of-UV-Visible-Spectrophotometer_fig1_327623886

[48] L. Herissi, Élaboration et caractérisation de couches minces d'oxydes métalliques destinées à des applications optoélectroniques, Thèse de doctorat en sciences,Université Larbi Ben M'hidi-Oum El Bouaghi (Algérie), 2016.

[49] https://www.researchgate.net/figure/Growth-sequence-dependent-film-thickness-and-optical-transmittance-a-The-growth_fig1_253495948

[50] H. Moualkia, Elaboration et Caractérisation de Couches Minces de Sulfure de Cadmium (CdS), Thèse de Doctorat, Université de Mentouri-Constantine (Algérie), 2010.

[51] S. Chelouche, Propriétés des fenêtres optiques ZnO:Al pour cellules solaires en couches minces à base de CIGS, Mémoire de Magister, Université Ferhat Abbas-Sétif (Algérie), 2012.

[52] F. Bouabida, Variation des propriétés structurales et optiques des couches minces de ZnO sous l'effet du temps de dépôts, Mémoire de master, Université Larbi Tébessi.Tébessa (Algérie), 2013.

[53] A. Bougrine, A. El Hichou, M. Addou, J. Ebothé, A. Kachouna, M. Troyon, Material Chemistry and Physics. 2003, 80, 438-445.

Abstract

Abstract

In recent years, significant studies have been conducted on transparent semiconducting oxide thin films. Due to their promising optical characteristics, high stability, and good electrical properties, n- or p-type semiconducting metal oxides are known as transparent conducting oxides . Among the various P-type semiconductors, nickel oxide is one with a direct band gap that varies between 3.6 and 4 eV depending on the deposition technique, and has attracted much attention due to its important applications in optoelectronic devices such as ultraviolet optoelectronic devices, energy efficient smart windows, positive electrodes in batteries, solar thermal absorbers, fuel cells, catalysts, in materials for gas or temperature sensors, such as CO sensor, H2 sensor, and formaldehyde sensors, in electrochromic display devices, and so on.

In this work, NiO will be deposited with various Zn-doping percentages (0, 1, 5, 10%), at a deposition temperature of 350 ̊C, according to the spray pyrolysis technique and with the use of solar energy as substrate heater.

Structural, optical and electrical characterization will be achieved. Those properties will be examined using X-ray diffraction (XRD) to investigate structural properties such as the crystalline quality and nature of the layers, grain size, dislocation density, and strain. UV-visible spectrophotometer will be used to analyse the optical characteristics such as the spectrum of the transmittance and the optical gap energy whereas the four probes method will be used to measure the electrical conductivity of the prepared samples.

Keywords: *transparent semiconducting oxide, P-type semiconductors, NiO, Zn-doping, spray pyrolysis technique, solar energy.*

Résumé

Ces dernières années, des études importantes ont été menées sur les couches minces d'oxydes semi-conducteurs transparents. En raison de leurs caractéristiques optiques prometteuses, de leur stabilité élevée et de leurs bonnes propriétés électriques, les oxydes métalliques semi-conducteurs de type n ou p sont connus sous le nom d'oxydes conducteurs transparents. Parmi les différents semi-conducteurs de type P, l'oxyde de nickel est celui dont la bande interdite directe varie entre 3,6 et 4 eV selon la technique de dépôt , et a attiré beaucoup d'attention en raison de ses applications importantes dans les dispositifs optoélectroniques tels que l'optoélectronique ultraviolette. intelligents, les fenêtres intelligentes écoénergétiques, les électrodes positives dans les batteries, les absorbeurs solaires thermiques, les piles à combustible, les catalyseurs, dans les matériaux pour les capteurs de gaz ou de température, tels que les capteurs de CO, les capteurs H2 et les capteurs de formaldéhyde, dans les dispositifs d'affichage électrochromiques, et bientôt.

Dans ce travail, NiO sera déposé avec différents pourcentages de dopage en Zn (0, 1, 5, 10%), à une température de dépôt de 350°C, selon la technique de pyrolyse par pulvérisation et avec l'utilisation de l'énergie solaire comme réchauffeur de substrat.

Une caractérisation structurale, optique et électrique sera réalisée. Ces propriétés seront examinées à l'aide de la diffraction des rayons X (XRD) pour étudier les propriétés structurelles telles que la qualité cristalline et la nature des couches, la taille des grains, la densité de dislocation et la déformation. Le spectrophotomètre UV-visible sera utilisé pour analyser les caractéristiques optiques telles que le spectre de la transmittance et l'énergie de l'écart optique tandis que la méthode des quatre sondes sera utilisée pour mesurer la conductivité électrique des échantillons préparés.

Mots-clés : *oxyde semi-conducteur transparent, semi-conducteurs de type P, NiO, dopage Zn, technique de pyrolyse par pulvérisation, énergie solaire.*

ملخص

في السنوات الأخيرة ، أجريت دراسات مهمة على أغشية رقيقة شفافة من أكسيد أشباه الموصلات. نظرًا لخصائصها البصرية الواعدة ، واستقرارها العالي ، وخصائصها الكهربائية الجيدة ، تُعرف أكاسيد الفلزات شبه الموصلة من النوع n أو p باسم أكاسيد التوصيل الشفافة . من بين أشباه الموصلات من النوع P ، يعتبر أكسيد النيكل واحدًا به فجوة نطاق مباشرة تتراوح بين 3.6 و 4 فولت اعتمادًا على تقنية الترسيب ، وقد جذب الكثير من الاهتمام نظرًا لتطبيقاته المهمة في الأجهزة الإلكترونية الضوئية مثل الأشعة فوق البنفسجية الإلكترونية الضوئية الأجهزة ، والنوافذ الذكية الموفرة للطاقة ، والأقطاب الكهربائية الموجبة في البطاريات ، والممتصات الحرارية الشمسية ، وخلايا الوقود ، والمحفزات ، في المواد الخاصة بأجهزة استشعار الغاز أو درجة الحرارة ، مثل مستشعر ثاني أكسيد الكربون ، ومستشعر H2 ، ومستشعرات الفورمالديهايد ، في أجهزة العرض الكهروضوئية ، و قريباً.

في هذا العمل ، سيتم ترسيب NiO بنسب مختلفة من منشطات الزنك (0 ، 1 ، 5 ، 10٪) ، عند درجة حرارة ترسيب 350 درجة مئوية ، وفقًا لتقنية الانحلال الحراري بالرش وباستخدام الطاقة الشمسية كمسخن ركيزة.

سيتم تحقيق الخصائص الهيكلية والبصرية والكهربائية. سيتم فحص هذه الخصائص باستخدام حيود الأشعة السينية (XRD) للتحقق من الخصائص الهيكلية مثل الجودة البلورية وطبيعة الطبقات وحجم الحبيبات وكثافة الخلع والانفعال. سيتم استخدام مقياس الطيف الضوئي المرئي بالأشعة فوق البنفسجية لتحليل الخصائص الضوئية مثل طيف النفاذية وطاقة الفجوة الضوئية بينما سيتم استخدام طريقة المجسات الأربعة لقياس التوصيل الكهربائي للعينات المعدة.

الكلمات المفتاحية: *أكسيد أشباه الموصلات الشفاف، أشباه الموصلات من النوع P، أكسيد النيكل، منشطات الزنك، تقنية الانحلال الحراري بالرش، الطاقة الشمسية.*